

CALIFORNIA CURRENT INTEGRATED ECOSYSTEM ASSESSMENT (CCIEA) CALIFORNIA CURRENT ECOSYSTEM STATUS REPORT, 2019

A report of the NOAA CCIEA Team to the Pacific Fishery Management Council, March 7, 2019.

*Editors: Dr. Chris Harvey (NWFSC), Dr. Toby Garfield (SWFSC), Mr. Greg Williams (PSMFC),
and Dr. Nick Tolimieri (NWFSC)*

1 INTRODUCTION

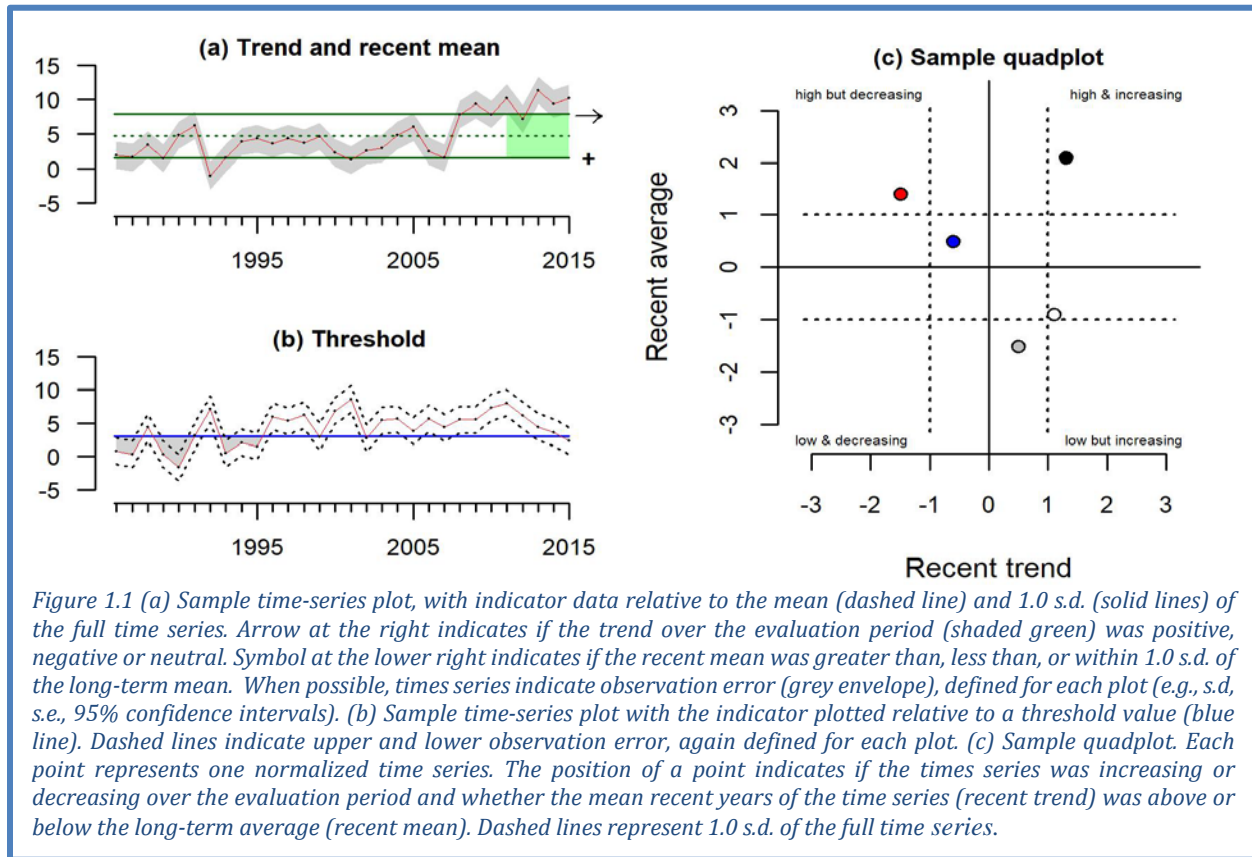
Section 1.4 of the 2013 Fishery Ecosystem Plan (FEP) established a reporting process wherein NOAA provides the Pacific Fishery Management Council (Council) with a yearly update on the status of the California Current Ecosystem (CCE), as derived from environmental, biological, economic and social indicators. NOAA's California Current Integrated Ecosystem Assessment (CCIEA) team is responsible for this report. This marks our 7th report, with prior reports in 2012 and 2014-2018.

This report summarizes CCE status based on data and analyses that generally run through 2018, with some projections for 2019 as well. Highlights are summarized in Box 1.1. Appendices provide additional information or clarification, as requested by the Council, the Scientific and Statistical Committee (SSC), or other advisory bodies.

Box 1.1: Highlights of this report

- **Climate, oceanographic and streamflow indicators were fairly near average in 2018, though indices suggest weakening circulation and emerging mild El Niño conditions**
- **Several ecological indicators in 2018 reflect average or improving conditions:**
 - The copepod community off Newport was predominately cool-water, lipid-rich species
 - Krill lengths off northern California have increased
 - Anchovy densities continued to increase
 - Several indicators of juvenile and adult salmon survival increased slightly, particularly for coho salmon in the northern part of the system
 - Sea lion pup numbers, sea lion pup growth, and piscivorous seabird densities were high
- **However, there was lingering evidence of unfavorable conditions in 2018:**
 - Warmer than average subsurface water in the southern portion of the system
 - Strong hypoxia on the shelf in the northern part of the system
 - Pyrosomes (warm-water tunicates) remained abundant in northern and central waters
 - Reports of whale entanglements in fixed fishing gear were high for the fifth straight year
- **West Coast fishery landings in 2017 increased by 27.4% over 2016; revenues increased by 12.3%. Increases were driven by Pacific hake, Dungeness crab and market squid**
- **Fishery diversification remains relatively low on average across all vessel classes**
 - We introduce estimates of shifting annual availability of groundfish to different ports
- **Forecasts for 2019 include:**
 - A 65% chance of a weak El Niño through at least the spring
 - Average coho returns to Oregon coast, below-average Chinook returns to the Columbia R.
 - Extensive hypoxia and acidified bottom waters over the shelf off Washington and Oregon

Throughout this report, most indicator plots follow the formats illustrated in Figure 1.1.

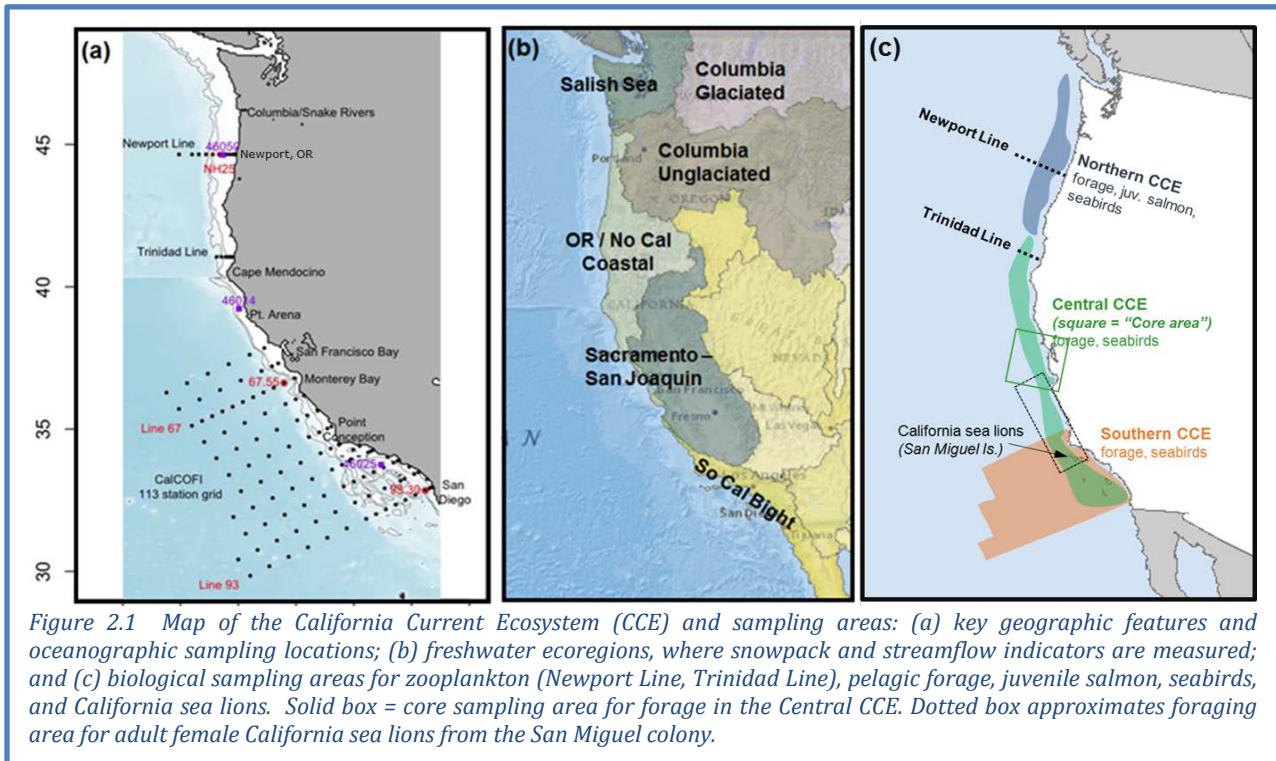


2 SAMPLING LOCATIONS

Figure 2.1a shows the CCE and headlands that define key biogeographic boundaries. We generally consider areas north of Cape Mendocino to be the “Northern CCE,” areas between Cape Mendocino and Point Conception the “Central CCE,” and areas south of Point Conception the “Southern CCE.” Figure 2.1a also shows sampling locations for most regional oceanographic data (Sections 3.2 and 3.3). Key transects are the Newport Line off Oregon, the Trinidad Line off northern California, and the CalCOFI grid further south. This sampling is complemented by basin-scale observations and models.

Freshwater ecoregions in the CCE are shown in Figure 2.1b, and are the basis by which we summarize indicators for snowpack, streamflow and stream temperature (Section 3.5).

Figure 2.1c indicates sampling locations for most biological indicators, including zooplankton (Section 4.1), forage species (Section 4.2), juvenile salmon (Section 4.3), California sea lions (Section 4.6) and seabirds (Section 4.7). The blue and green areas in Figure 2.1c also approximate the areal extent of the groundfish bottom trawl survey (Section 4.4), which covers trawlable habitat on the shelf and upper slope (55–1280 m depths). Indicators of highly migratory species (HMS, Section 4.5) are derived from data collected at scales far larger than pictured in Figure. 2.1c.



3 CLIMATE AND OCEAN DRIVERS

Climate and ocean indicators in the CCE in 2018 reveal a physical system that remains in transition following the historically unprecedented marine heat wave from 2014-2015 and the strong El Niño event in 2015-2016. The transition is visible in Figure 3.1, where ocean temperature anomalies appear milder over the last two years than the years preceding. In 2018, nearshore sampling stations in the northern and southern CCE began the year with temperature anomalies near the long-term mean. Temperature anomalies in the north (station NH25) were less than 0.5°C, and progressively cooled near the surface to neutral or small negative anomalies (~-0.5°C). The southern station (CalCOFI 93.30) had the opposite temperature progression, with temperatures in the upper 100 m increasing and reaching the largest warm anomalies for the year by October 2018. This temperature increase was attributed to an influx of warm offshore waters (Thompson et al. 2018). This reverses a pattern described in last year's report, when subsurface anomalies in late 2016-2017 were slightly positive in the north and cooler in the south.

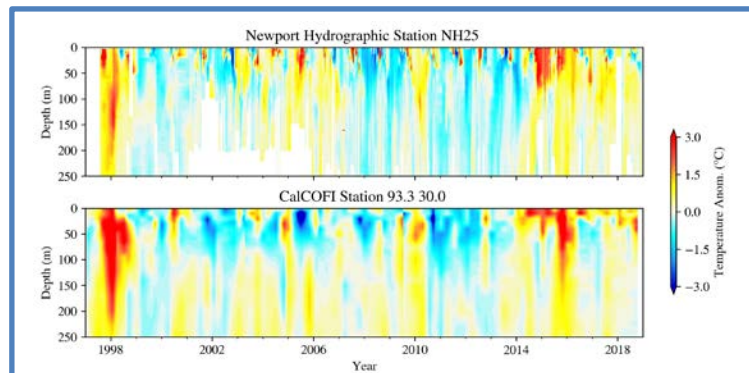
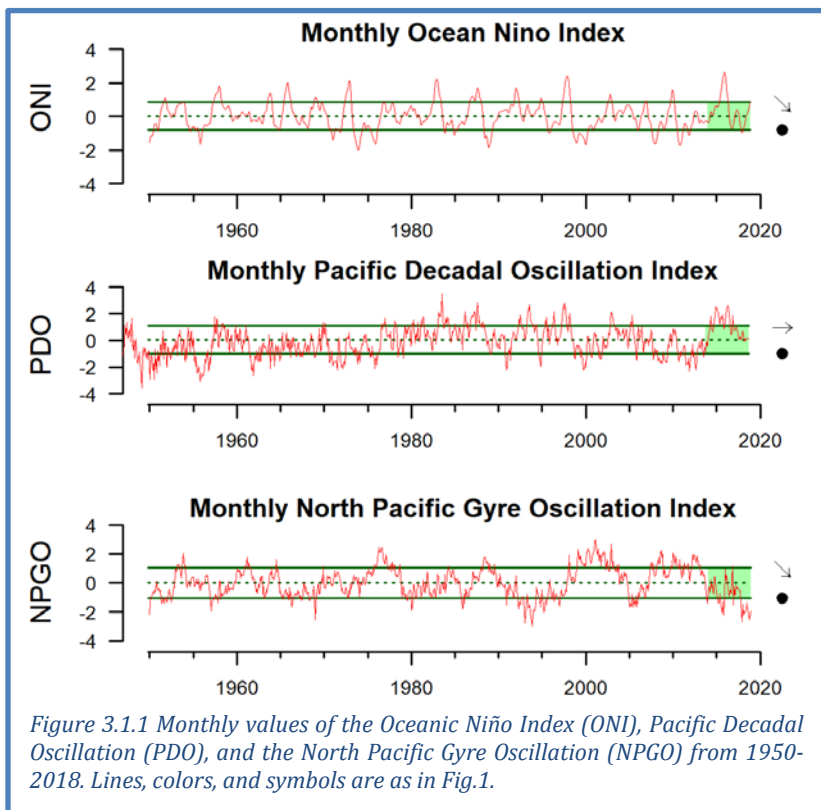


Figure 3.1 Time-depth temperature anomaly contours for nearshore stations NH25 (August 1998 to September 2018) and CalCOFI 93.30 (January 1998 to August 2018). For location of these stations see Fig. 2.1a. Extreme warm anomalies occurred throughout the water column during El Niño events in 1998 and 2016 and at the surface in the marine heat wave of 2014-2015. Off Newport, surface waters cooled in 2018, while water below 50 m remained above the long-term average. In the south, water throughout the water column remained above average.

3.1 BASIN-SCALE INDICATORS

To describe a wide range of large-scale physical ecosystem states, we report three independently varying indices. The Oceanic Niño Index (ONI) describes the equatorial El Niño Southern Oscillation (ENSO). A positive ONI indicates El Niño conditions, which usually mean lower primary productivity, weaker upwelling, poleward transport of equatorial waters and species, and more storms to the south in the CCE. A negative ONI means La Niña conditions, which usually lead to higher productivity. The Pacific Decadal Oscillation (PDO) describes Northeast Pacific sea surface temperature anomalies (SSTa) that may persist for many years. Positive PDOs are associated with warmer waters and lower productivity in the CCE, while negative PDOs indicate cooler waters and higher productivity. The North Pacific Gyre Oscillation (NPGO) is a signal of sea surface height, indicating changes in ocean circulation that affect source waters for the CCE. Positive NPGOs are associated with increased equatorward flow and higher surface salinities, nutrients, and chlorophyll-*a*. Negative NPGOs are associated with decreases in such values, less subarctic source water, and lower CCE productivity.

In 2018, the ONI transitioned from the negative values of 2017 to neutral or weak El Niño conditions in the equatorial Pacific as of January 2019 (Figure 3.1.1, top). The Climate Prediction Center forecasts a ~65% chance for a weak El Niño to develop in spring 2019. The PDO has experienced a downward trend from high positive values over the last five years, reaching the long-term mean in 2018 (Figure 3.1.1, middle). This indicates that sea surface temperatures have steadily decreased from the extremes of the marine heat wave (Bond et al. 2015). However, the NPGO has declined to near historic lows over the last five years (Figure 3.1.1, bottom). This indicates an ongoing weak influx of nutrient-rich water from the North Pacific; the negative NPGO and a possible weak El Niño could represent a constraint on productivity in the CCE. Seasonal values for basin-scale indices are in Appendix D.1.



In 2018, large positive SSTa were mostly seen within the Southern California Bight during winter and summer (Figure 3.1.2, left). Average SSTa from 2014-2018 were positive for the majority of the eastern North Pacific, with means above 1 s.d. occurring over large areas including the Gulf of Alaska and the Southern California Bight (Figure 3.1.2, middle). These elevated 5-year mean SSTa are driven primarily by the 2014-2015 marine heat wave and the 2016 El Niño event (Jacox et al. 2016). SST cooled during 2017 and 2018; the widespread cooling trends (Figure 3.1.2, right) reflect the return to more average conditions after the extreme heating.

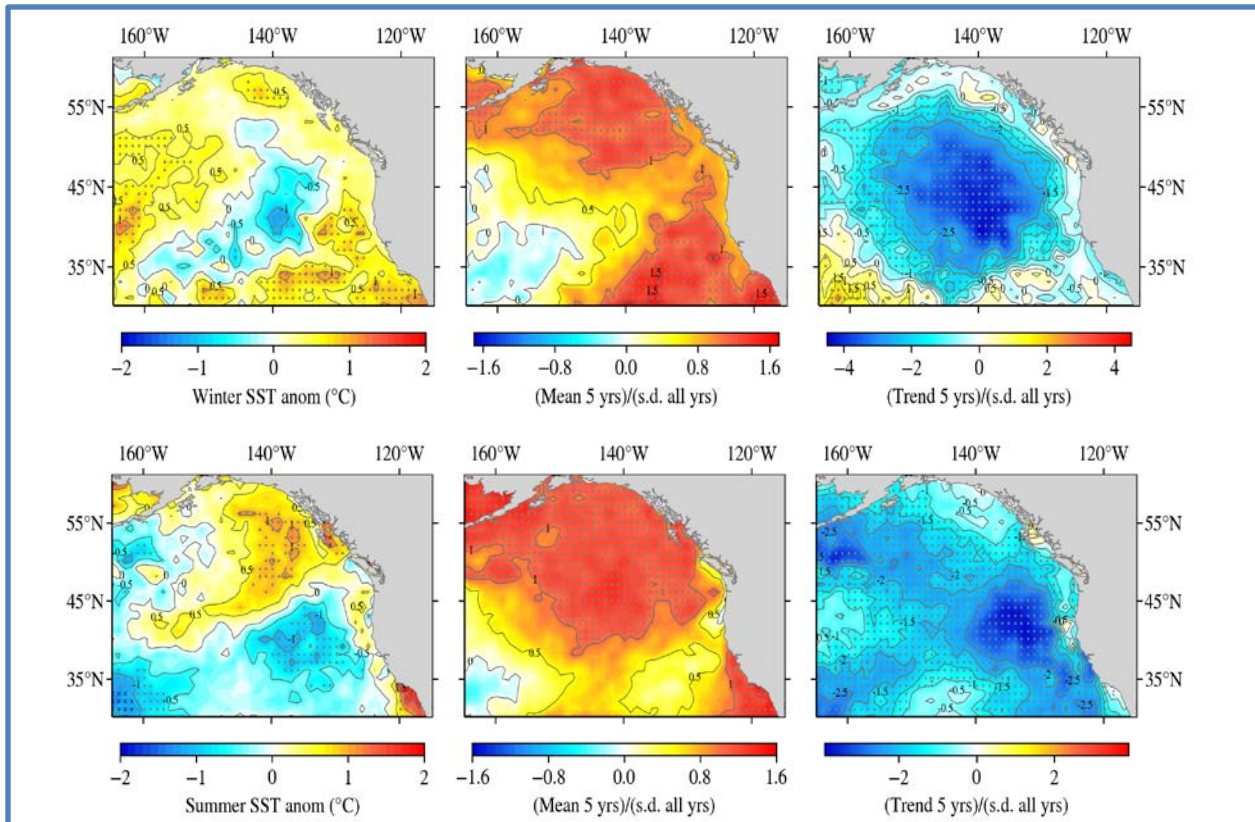


Figure 3.1.2 Left: Sea surface temperature (SST) anomalies in 2018, based on 1982-present satellite time series in winter (Jan-Mar; top) and summer (July-Sept; bottom); the 2018 summer warming of the Southern California Bight is evident. Center: Mean SST anomalies for 2014-2018. Right: trends in SST anomalies from 2014-2018, which are mostly negative because the marine heat wave of 2014-2015 and major El Niño of 2016 have subsided. Black circles mark cells where the anomaly was > 1 s.d. above the long-term mean. Black x's mark cells where the anomaly was the highest in the time series.

In late 2018, news media reported that, based on satellite imagery of SSTa, a marine heatwave similar to the “Blob” of 2014-2015 may be reforming in the northeast Pacific. Based on an analysis of SSTa from 1985-2016 (Leising, in prep), a marine heatwave has the potential to cause coastal impacts similar to those from the 2014-2015 event if the anomalous feature: (1) has SSTa > 2 s.d. of the long-term SSTa time series at a particular location; (2) is greater than 500,000 km² in area; and (3) lasts for > 60 days. The feature in late 2018 (Figure 3.1.3) surpassed the area threshold, but did not surpass

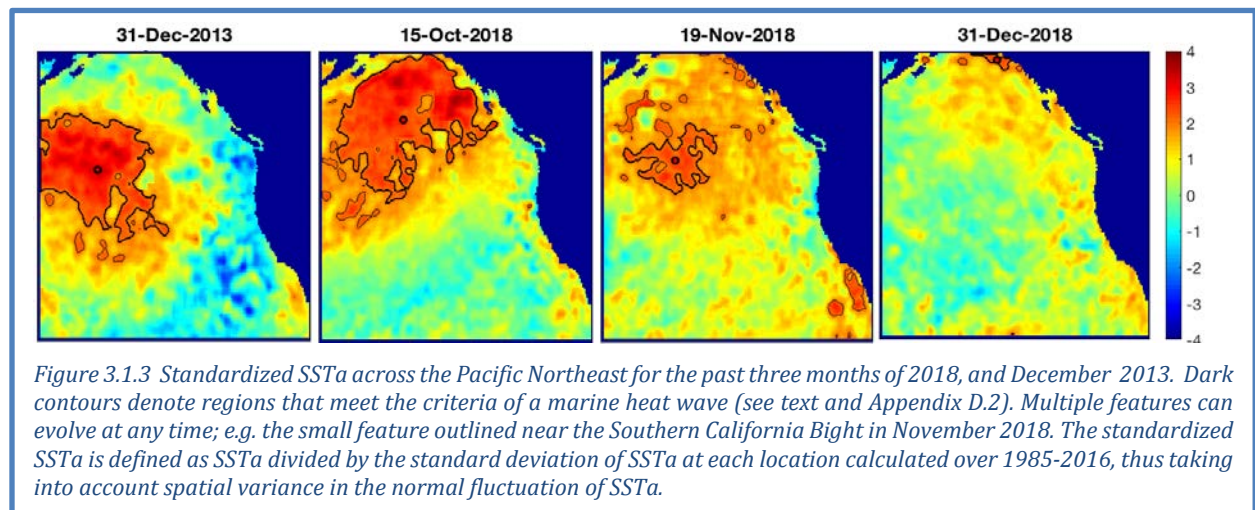


Figure 3.1.3 Standardized SSTa across the Pacific Northeast for the past three months of 2018, and December 2013. Dark contours denote regions that meet the criteria of a marine heat wave (see text and Appendix D.2). Multiple features can evolve at any time; e.g. the small feature outlined near the Southern California Bight in November 2018. The standardized SSTa is defined as SSTa divided by the standard deviation of SSTa at each location calculated over 1985-2016, thus taking into account spatial variance in the normal fluctuation of SSTa.

the duration threshold (see Appendix D.2). Moreover, it largely dissipated by December 2018 (unlike December 2013, prior to the 2014-2015 “Blob” event; Figure 3.1.3, left). The CCIEA team believes that a large-scale marine heatwave is not currently affecting the northeast Pacific or the CCE, although SSTa currently remains positive and conditions may change. Additional information on this analysis is in Appendix D.2.

3.2 REGIONAL CLIMATE INDICATORS

Upwelling, driven by variation in wind stress, is a physical process that moves cold, nutrient-rich water from deep in the ocean to the surface layer, which fuels the high seasonal primary production at the base of the CCE food web. The most common metric of upwelling is the Bakun Upwelling Index (UI), reported at a spatial scale of 1° latitude x 1° longitude. However, the Bakun UI does not take into consideration the underlying ocean structure (e.g. ocean stratification), which can have considerable influence on the volume and the nutrient content of the upwelled water. Jacox et al. (2018) developed new estimates of coastal upwelling using ocean models to improve upon the Bakun UI by estimating the vertical transport (Cumulative Upwelling Transport Index; CUTI) and nitrate flux (Biologically Effective Upwelling Transport Index; BEUTI).

The magnitude of vertical nitrate flux in the CCE varies greatly by latitude (Figure 3.2.1, left). The northern stations at 45°N (Newport, OR) and 39° (Point Arena, CA) undergo downwelling in the winter due to reversing winds. The nitrate flux at 39°N is much greater than at 33° (Southern California) and 45°N. The timing of peak upwelling varies by latitude, with northern latitudes having a later onset of maximum upwelling. This can be seen in the maximum climatological value of CUTI, which is at the end of April at 33°N, the middle of June at 39°N, and the end of July at 45°N (Figure 3.2.1;). During 2018, BEUTI and CUTI were generally average through most of the seasons, with strong periods of upwelling during the spring at 33° and 39°N. In general, CUTI and BEUTI show similar fluctuations in the north and less in the south. In the southern latitudes BEUTI is more influenced by subsurface nutrient concentration.

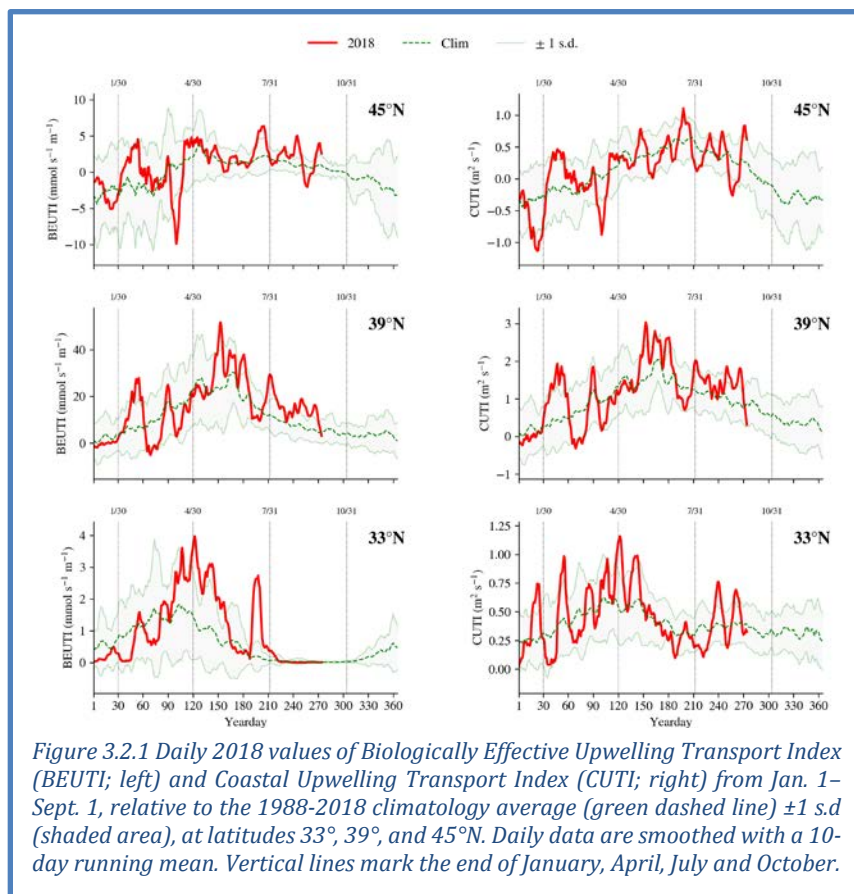


Figure 3.2.1 Daily 2018 values of Biologically Effective Upwelling Transport Index (BEUTI; left) and Coastal Upwelling Transport Index (CUTI; right) from Jan. 1–Sept. 1, relative to the 1988-2018 climatology average (green dashed line) ± 1 s.d. (shaded area), at latitudes 33°, 39°, and 45°N. Daily data are smoothed with a 10-day running mean. Vertical lines mark the end of January, April, July and October.

3.3 HYPOXIA AND OCEAN ACIDIFICATION

Dissolved oxygen (DO) is dependent on processes such as currents, upwelling, air-sea exchange, community-level production, and respiration. Low DO can compress habitat and cause stress or die-offs for sensitive species. Waters with DO levels <1.4 ml/L (2 mg/L) are considered hypoxic.

For the second consecutive year, low DO was a serious issue in the northern CCE. At station NH05 (5 km off of Newport, OR), water near bottom over the continental shelf was below the hypoxia threshold from June through September before its seasonal rebound in fall (Figure 3.3.1, top). Hypoxic DO levels were also observed during June further offshore at station NH25 (Figure 3.3.1, bottom). Seasonal trends for these stations and other stations off Southern California (where DO was well above the 1.4 ml/L threshold) are shown in Appendix D.3.

Ocean acidification (OA), caused by increased levels of atmospheric CO₂, lowers pH and carbonate in seawater. An indicator of OA is the saturation state of aragonite (a form of calcium carbonate). Aragonite saturation <1.0 indicates corrosive conditions that may be stressful to shell-forming organisms and other species. Upwelling transports hypoxic, acidified waters from offshore onto the continental shelf, where increased community-level metabolic activity can further exacerbate OA (Chan et al. 2008, Feely et al. 2008).

Aragonite saturation levels off Newport in 2018 had some of the lowest values over the last five years (Figure 3.3.2). At the nearshore station (NH05), aragonite levels at 50 m depth were saturated (>1.0) in winter and spring, then fell below 1.0 in the summer and fall, as is typical, although summer/fall values were lower than in the anomalous years of 2014-2016, implying greater extent of OA in 2018. At station NH25 at 150 m depth, aragonite saturation state followed the same seasonal cycle but across a narrower range; conditions at this site and depth were always corrosive (<1.0). Seasonal aragonite trends are in Appendix D.3.

3.4 HARMFUL ALGAL BLOOMS

In response to requests from various Council advisory bodies, this year we are introducing a new indicator of the occurrence of harmful algal blooms (HABs). Blooms of the diatom genus *Pseudo-nitzschia* can increase concentrations of the toxin domoic acid in coastal waters. Because domoic acid can cause amnesic shellfish poisoning in humans, shellfish fisheries (including the recreational razor clam and commercial Dungeness crab fisheries) are closed when concentrations exceed regulatory thresholds for human consumption. Razor clams provide an accurate record of the arrival and intensity of HAB events on beaches, and they can accumulate and retain domoic acid for up to a year following HABs of *Pseudo-nitzschia*. Extremely toxic HABs of *Pseudo-nitzschia* frequently coincide with warming events in the CCE (Appendix E).

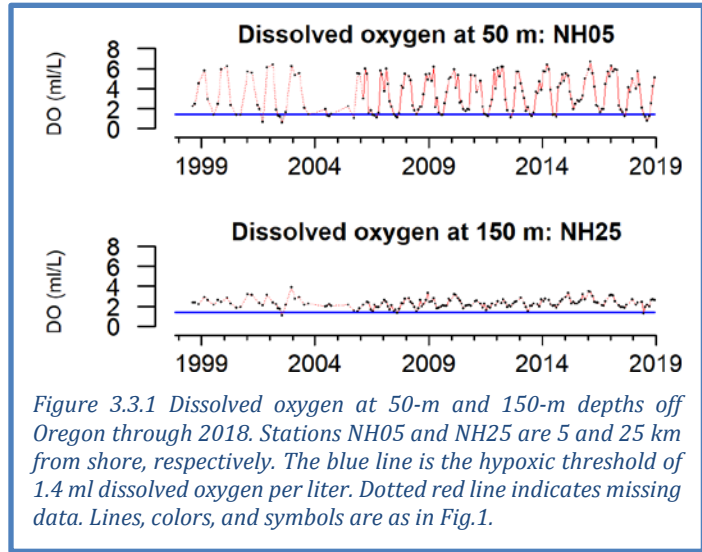


Figure 3.3.1 Dissolved oxygen at 50-m and 150-m depths off Oregon through 2018. Stations NH05 and NH25 are 5 and 25 km from shore, respectively. The blue line is the hypoxic threshold of 1.4 ml dissolved oxygen per liter. Dotted red line indicates missing data. Lines, colors, and symbols are as in Fig.1.

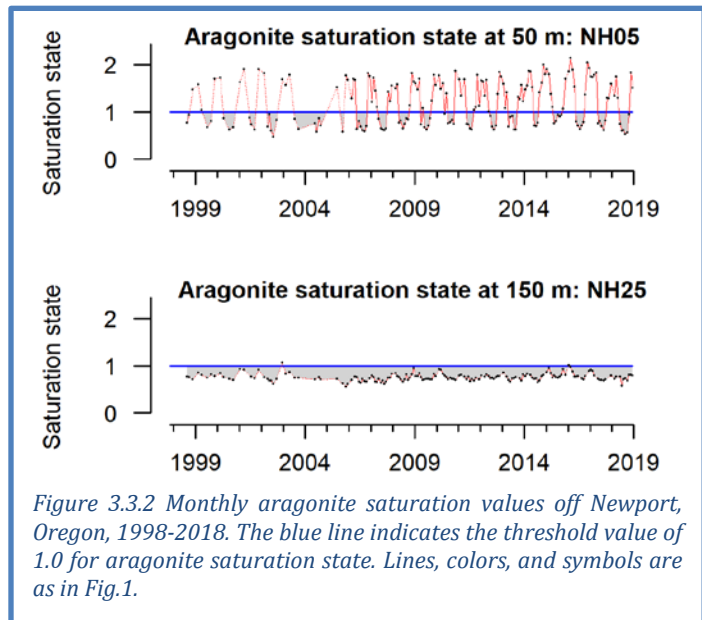


Figure 3.3.2 Monthly aragonite saturation values off Newport, Oregon, 1998-2018. The blue line indicates the threshold value of 1.0 for aragonite saturation state. Lines, colors, and symbols are as in Fig.1.

Monthly maximum domoic acid concentrations in razor clams from six sites along the Washington coast from 1991 through 2018 are shown in Figure 3.4.1; site-specific trends are in Appendix E. Domoic acid levels at or exceeding 20 parts per million trigger closures of razor clam harvests; such events occurred most recently in 2015, 2016 and 2017, coincident with the anomalous warming events in the CCE. In 2018, the low levels of domoic acid detected in Washington razor clams and Dungeness crabs did not trigger fishery closures at any of the sites.

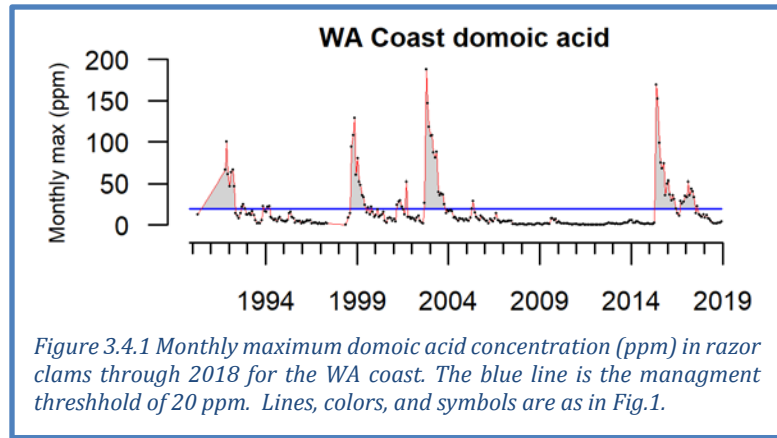


Figure 3.4.1 Monthly maximum domoic acid concentration (ppm) in razor clams through 2018 for the WA coast. The blue line is the management threshold of 20 ppm. Lines, colors, and symbols are as in Fig.1.

3.5 HYDROLOGIC INDICATORS

Freshwater conditions are critical for salmon populations and estuaries that support many marine species. The indicators presented here include snowpack, streamflow and stream temperature, summarized by freshwater ecoregion (see Figure 2.1b) or by salmon evolutionarily significant units (ESUs, Waples 1995). Snow-water equivalent (SWE) is the water content in snowpack, which provides cool freshwater in the spring, summer and fall months. Maximum streamflow in winter and spring is important for habitat formation and removal of parasites, but extreme discharge relative to historic averages can scour salmon nests (redds). Minimum streamflow in summer and fall can restrict habitat for in-stream juveniles and migrating adults. High summer water temperatures can impair physiology and cause mortality to both juveniles and adults. All indicators are influenced by climate and weather patterns and will be affected as climate change intensifies.

In 2018, SWE anomalies were within 1 s.d. of long-term means, though the southerly ecoregions were relatively low (Figure 3.5.1). Even these ecoregions were well above the extremely low SWE

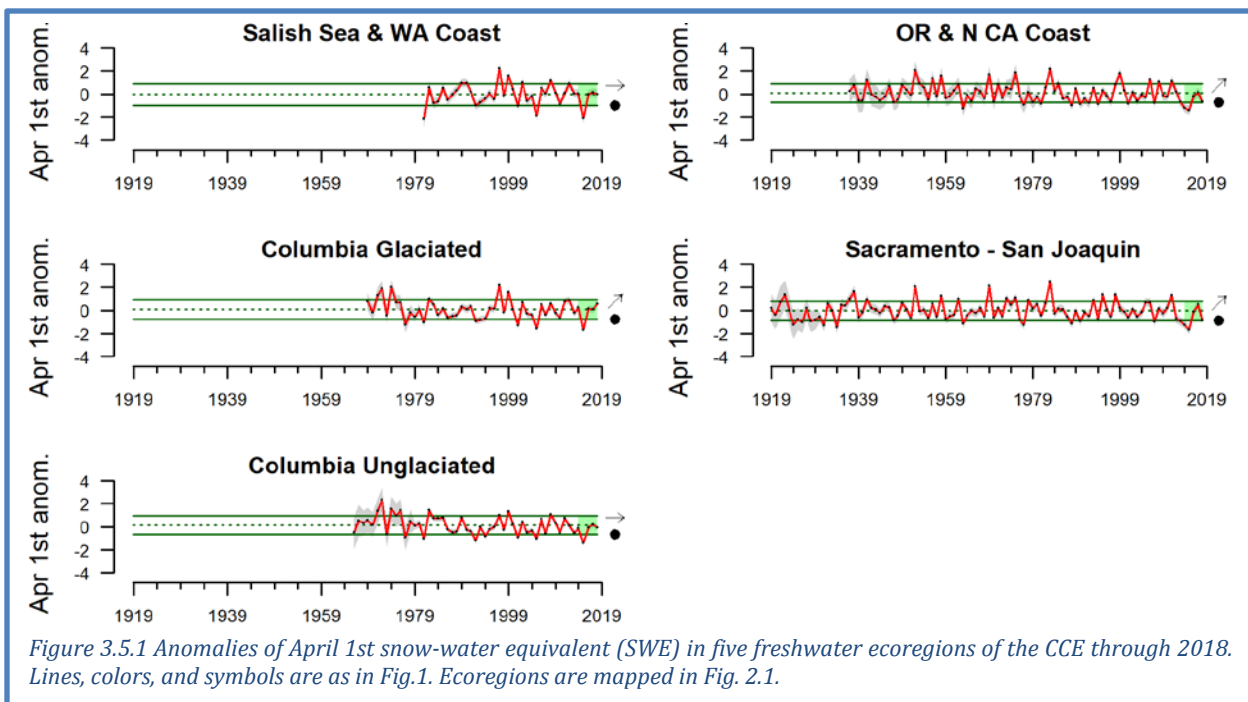
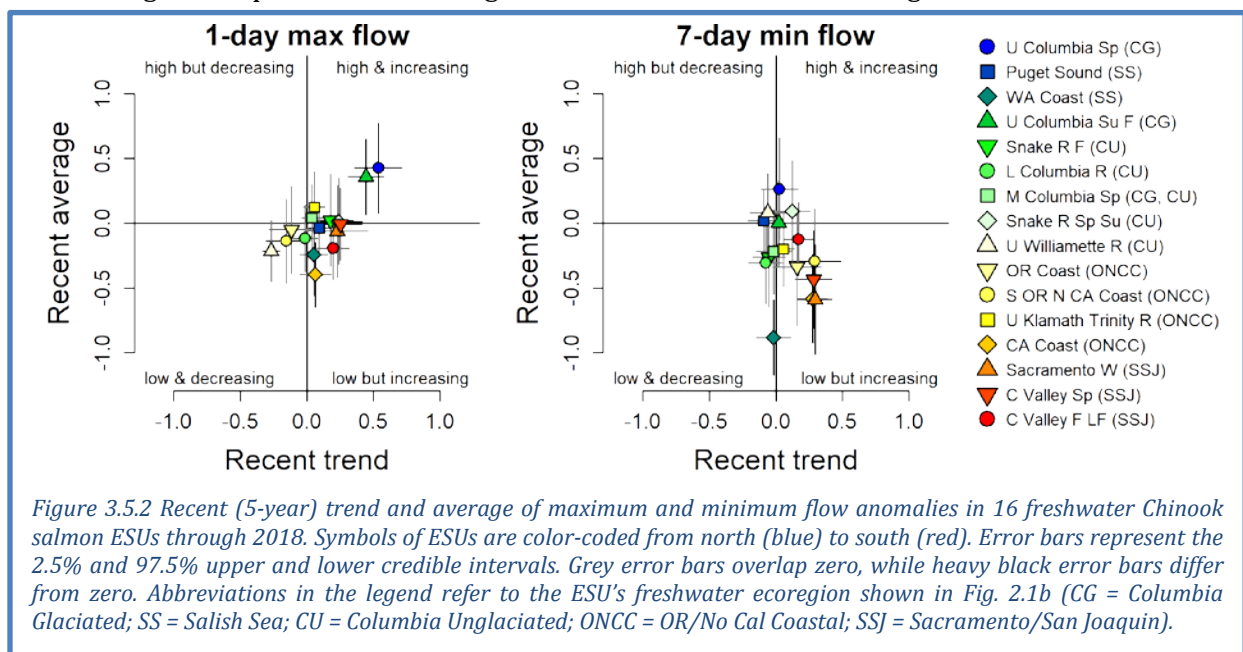


Figure 3.5.1 Anomalies of April 1st snow-water equivalent (SWE) in five freshwater ecoregions of the CCE through 2018. Lines, colors, and symbols are as in Fig.1. Ecoregions are mapped in Fig. 2.1.

measures of 2015. Corresponding to these precipitation patterns, minimum streamflows in 2018 were within 1 s.d. of long-term means in all ecoregions except the Southern California Bight, which was 1 s.d. below average (Appendix F). Maximum flows were at or above long-term means in the northerly ecoregions, but at or below average in the central and southerly ecoregions (Appendix F).

As of February 1st, SWE in 2019 is on pace to be below average in much of Washington, Oregon and Idaho, but above average in the Sierra Nevada range following high snow accumulation in January (Appendix F). Because SWE values do not typically peak until early spring, however, the peak measure of SWE for the year will not be until April 1, 2019.

We further summarized streamflows with quad plots that compile recent flow anomalies at the finer spatial scale of individual Chinook salmon ESUs. The error bars describe 95% credible intervals of flow, allowing us to determine which ESUs have significant short-term trends or recent averages that differ from long-term means. Maximum flow events were generally within range of long-term means, although the short-term trends of several ESUs were positive and some short term averages were greater than long-term means (Figure 3.5.2, left; Appendix F). The positive trends likely reflect short-term rebounds from the system-wide extremely low snowpack of 2015. Similarly, minimum flow anomalies had either positive or neutral short-term trends for all Chinook salmon ESUs that we evaluated (Figure 3.5.2, right). Recent averages of minimum flows were generally similar to long-term averages, except for below-average minimum flows for the Washington Coast ESU.



Maximum August stream temperatures, which are summarized by ecoregion in Appendix F, have been above average recently in the Salish Sea and Washington Coast ecoregion, and have experienced short-term declines along the Oregon Coast and in California following peaks in 2014-2016.

4 FOCAL COMPONENTS OF ECOLOGICAL INTEGRITY

The CCIEA team examines many indicators related to the abundance and condition of key species and the dynamics of ecological interactions and community structure. Many CCE species and processes respond very quickly to changes in ocean and climate drivers, while other responses may not manifest for many years. These dynamics are challenging to predict. From 2014 to 2016, the marine heatwave and major El Niño event resulted in generally poor productivity at lower trophic levels and poor foraging conditions for many predators. In 2017-2018, the physical and ecological influence of

these anomalous warm events lingered, although some ecological integrity indicators suggested a return toward average conditions, particularly in the southern CCE.

4.1 COPEPOD BIOMASS ANOMALIES AND KRILL SIZE

Copepod biomass anomalies represent inter-annual variation for two groups of copepod taxa: northern copepods, which are cold-water species rich in wax esters and fatty acids that appear to be essential for pelagic fishes; and southern copepods, which are warm-water species that are smaller and have lower fat content and nutritional quality. In summer, northern copepods usually dominate the coastal zooplankton community observed along the Newport Line (Figure 2.1a,c), while southern copepods dominate in winter. El Niño events and positive PDO regimes can promote higher biomass of southern copepods (Keister et al. 2011, Fisher et al. 2015). Positive values of northern copepods in summer are correlated with stronger returns of Chinook salmon to Bonneville Dam, and values >0.2 are associated with better survival of coho salmon (Peterson et al. 2014).

From the onset of the anomalous warm period in fall 2014 until mid 2017, copepod anomaly trends strongly favored southern copepods. However, in July 2017 the northern copepod anomaly shifted from negative to neutral, and has oscillated around neutral values ever since, while the southern copepod anomaly declined from positive to neutral values in 2017 and negative values by the end of 2018 (Figure 4.1.1). These changes seem to signal improving foraging conditions for pelagic fishes in this region of the CCE, relative to the anomalous period of 2014-2016.

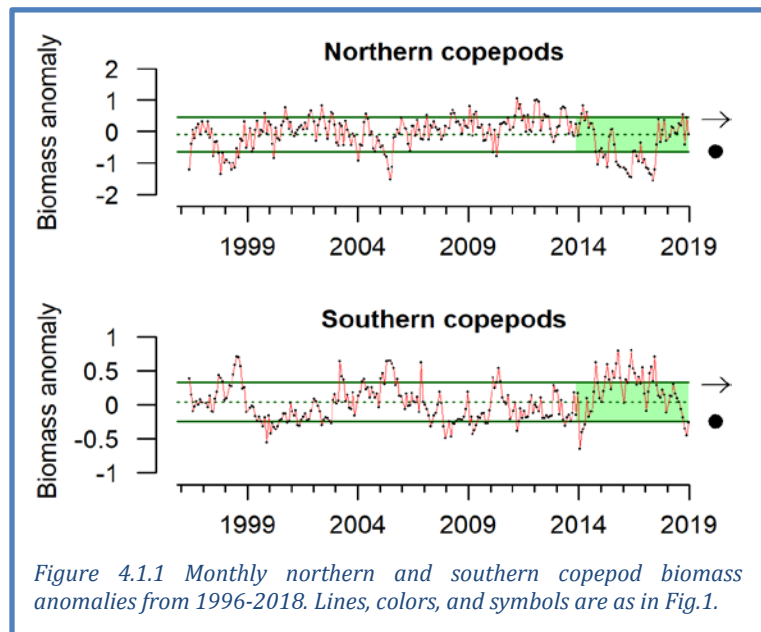


Figure 4.1.1 Monthly northern and southern copepod biomass anomalies from 1996-2018. Lines, colors, and symbols are as in Fig.1.

We added an additional indicator of lower trophic level productivity—the length of krill sampled on the Trinidad transect off northern California (41°N; Figure 2.1a,c). Zooplankton data at Trinidad indicated a shift in 2017-2018 toward species assemblages and conditions last observed prior to the 2014-2016 anomalies. One indicator of this is mean lengths of the cool-water krill *Euphausia pacifica*, an important prey item. Krill lengths were >1 s.d. below average for much of 2014-2016, but increased in the 2017 upwelling season and remained near or above the time series mean throughout much of 2017 and 2018 (Figure 4.1.2). Krill size naturally decreases in winter, but wintertime lengths in 2017 and 2018 were typical of pre-heat wave conditions. As with copepod community composition off Newport, these results imply more productive conditions for predators of zooplankton over the last two years.

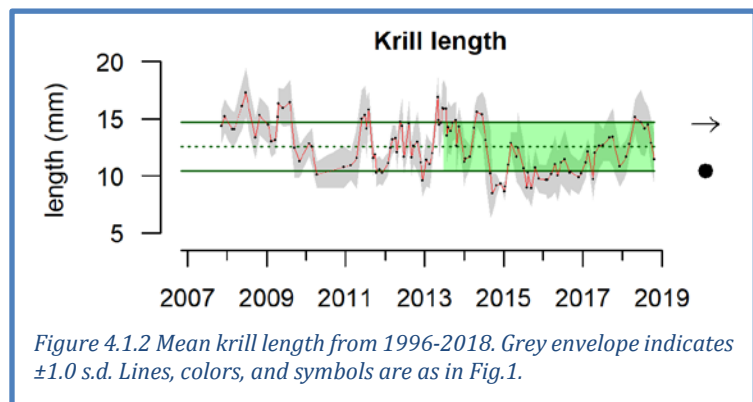


Figure 4.1.2 Mean krill length from 1996-2018. Grey envelope indicates ± 1.0 s.d. Lines, colors, and symbols are as in Fig.1.

4.2 REGIONAL FORAGE AVAILABILITY

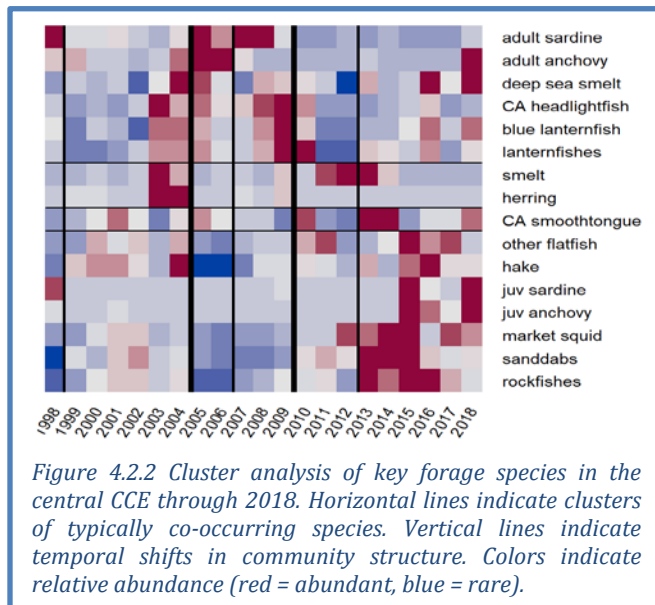
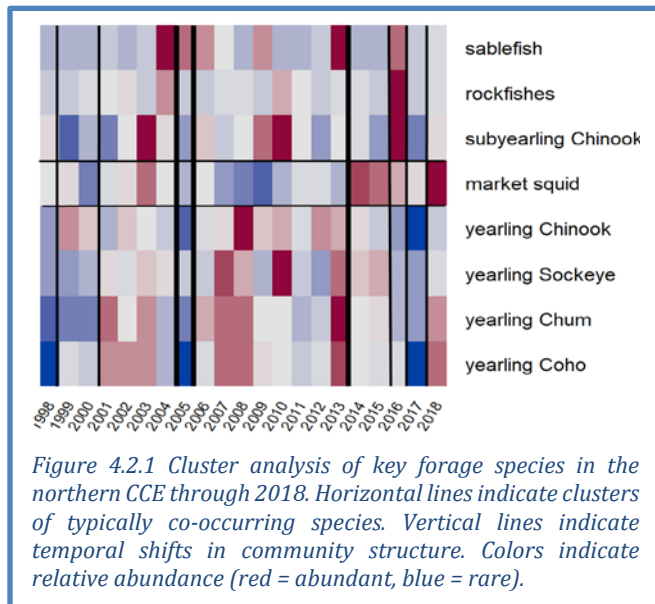
The CCE forage community is a diverse portfolio of species and life history stages, varying in behavior, energy content, and availability to predators. The species summarized here represent a substantial portion of the available forage in the CCE. *We consider these regional indices of relative forage availability and variability, not indices of abundance of coastal pelagic species (CPS).*

The regional surveys that produce CCE forage data use different methods (e.g., gear, timing, survey design), which makes comparisons across regions difficult. The CCIEA team has adopted new methods to identify and compare regional shifts in forage community composition. The new plots are shown here, with related time series plots in Appendix G. Clusters of co-occurring species are grouped on the y-axis and their regional abundances are indicated by color (red = abundant, blue = rare); significant temporal shifts in a region’s forage community composition are marked by vertical lines.

Northern CCE: The northern CCE survey off Washington and Oregon (Figure 2.1c) targets juvenile salmon in surface waters, but also effectively catches surface-oriented juvenile groundfish and squid. Since the major shift in the forage assemblage between 2013 and 2014, the assemblage has been variable, with minor shifts in each of the past 3 years (Figure 4.2.1). Market squid have been consistently present since 2014, while pelagic juvenile groundfish and salmon have been present intermittently. This departs from the 2006-2013 assemblage that was characterized by abundant salmon and very few market squid.

Central CCE: Data presented here are from the “Core area” of a survey (Figure 2.1c) that targets young-of-the-year (YOY) rockfishes, but also effectively samples pelagic fish and squid. This forage community last underwent a major shift before 2010, driven by the steep decline of adult sardines (Figure 4.2.2; see also Appendix G.2). A minor shift occurred between 2012 and 2013, as YOY rockfishes, YOY sanddabs, market squid, and many mesopelagic schooling fishes greatly increased and remained high through 2018. Other forage groups have occasionally been abundant during the 2013-2018 phase, including juvenile sardine, juvenile anchovy and adult anchovy in 2018.

Southern CCE: Forage data for the Southern CCE (Figure 2.1c) come from CalCOFI larval fish surveys. Larval biomass of forage species is assumed to correlate with regional abundance of adult forage species. The southern forage assemblage is the most variable over time, with 9 substantial breaks from 1998-



2018. The last major change was between 2011 and 2012, when sardine became very rare and larval rockfishes, flatfishes, squid and certain mesopelagic species became abundant (Figure 4.2.3; see also Appendix G.3). The assemblage was dynamic from 2014-2018, with spikes in mackerels in some years, squid and groundfishes in some years, and the recent increase in larval anchovy.

Many of these forage surveys have captured high numbers of pyrosomes, a type of warm-water gelatinous tunicate, ever since the anomalous warm years (Brodeur et al. 2018). Preliminary information from 2018 (data not shown) indicates that pyrosomes remained abundant in central and northern waters of the CCE, particularly earlier in the spring and summer, although densities in many areas appeared to be lower than in 2017.

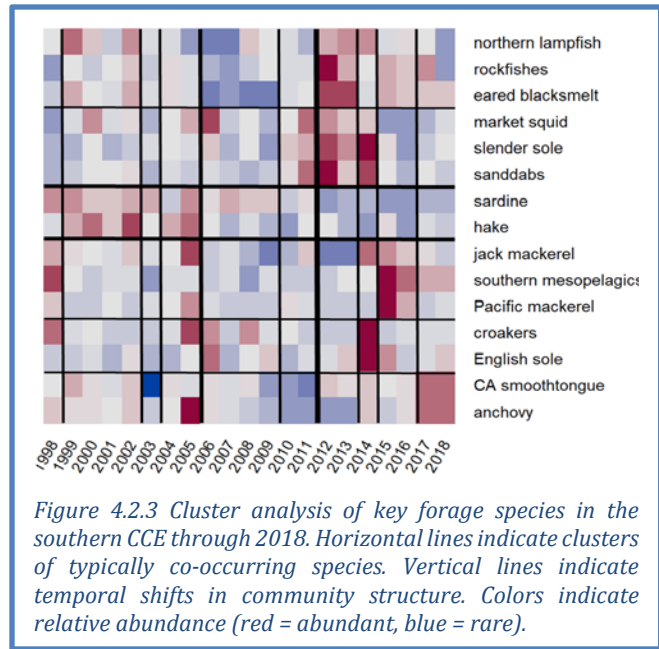


Figure 4.2.3 Cluster analysis of key forage species in the southern CCE through 2018. Horizontal lines indicate clusters of typically co-occurring species. Vertical lines indicate temporal shifts in community structure. Colors indicate relative abundance (red = abundant, blue = rare).

4.3 SALMON

For indicators of the abundance of adult Chinook salmon, we examine trends in natural spawning escapement from different populations to compare status and coherency in production dynamics across their range. We summarize escapement trends in quad plots; time series are shown in Appendix H. For juvenile salmon, we include time series of juvenile coho and Chinook salmon catches from surveys in the Northern CCE (Figure 2.1c).

Most Chinook salmon escapement data are updated through 2017. Generally, escapements of California Chinook salmon ESUs over the last decade of available data were within 1 s.d. of long-term averages (Figure 4.3.1), although 2017 escapements were among the lowest on record in several ESUs (Appendix H.1). California Chinook salmon stocks had neutral trends over the last decade, and annual variation was generally high (Appendix H.1). In Washington, Oregon and Idaho, most escapements were within 1 s.d. of average for the past decade; the exception was Snake River Fall Chinook after a series of large escapements since 2009 (Appendix H.2). Escapements in 2017 ranged from relatively high (Willamette Spring) to relatively low (Upper Columbia Spring, Lower Columbia; Appendix H.2). Escapement trends for northern stocks were mostly neutral, but Willamette Spring and Snake River Fall Chinook had significantly positive trends over the most recent decade of data.

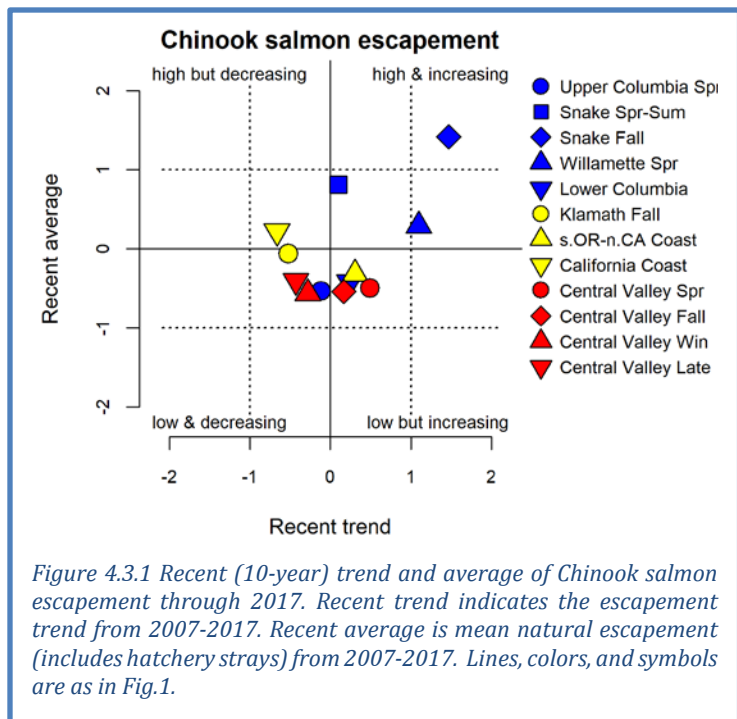


Figure 4.3.1 Recent (10-year) trend and average of Chinook salmon escapement through 2017. Recent trend indicates the escapement trend from 2007-2017. Recent average is mean natural escapement (includes hatchery strays) from 2007-2017. Lines, colors, and symbols are as in Fig.1.

Catches of juvenile Chinook and coho salmon in June off the coasts of Washington and Oregon can serve as indicators of survival during their first few weeks at sea, and are correlated to later years' returns of adults to Bonneville Dam. Catches of subyearling Chinook and yearling Chinook salmon were close to long-term averages in 2018, one year removed from near-historic lows; catches of yearling coho in 2018 were among the highest observed (Figure 4.3.2). These data suggest that the direct negative impacts of the marine heatwave on salmon survival have subsided. However, other aspects of the ecosystem have not completely returned to normal, suggesting that indirect impacts on survival may still occur. The recent catch trend for yearling Chinook in this region remains negative, while trends for subyearling Chinook and yearling coho salmon are neutral and more variable.

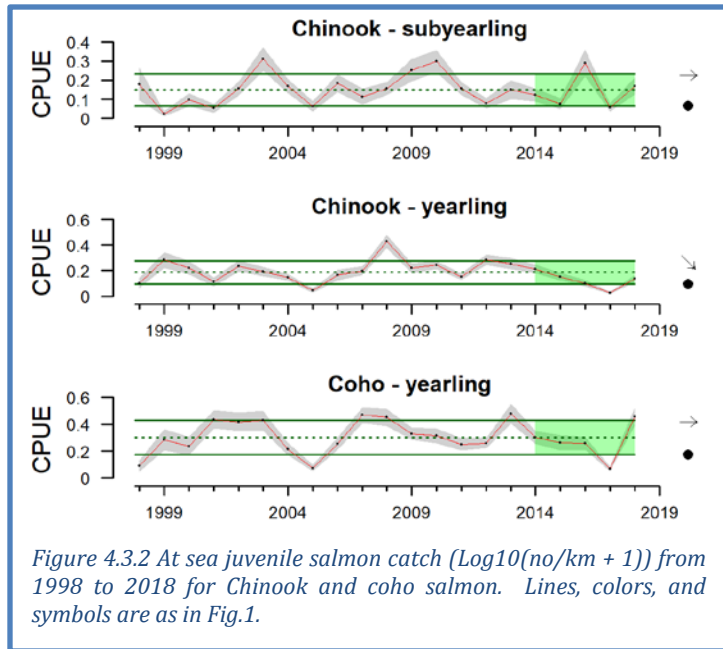


Figure 4.3.2 At sea juvenile salmon catch ($\text{Log}_{10}(\text{no}/\text{km} + 1)$) from 1998 to 2018 for Chinook and coho salmon. Lines, colors, and symbols are as in Fig.1.

A suite of relevant indicators suggests some improvements in returns of salmon to the Columbia Basin in 2019. Long-term associations between oceanographic conditions, food web structure, and salmon productivity (Burke et al. 2013, Peterson et al. 2014) support forecasts of returns of Chinook salmon to Bonneville Dam and smolt-to-adult survival of Oregon Coast coho salmon. Indicators of conditions for smolts that went to sea between 2015 and 2018 are generally consistent with below-average returns of Chinook and average returns of coho salmon in 2019, as depicted in the “stoplight chart” in Table 4.3.1; this includes many indicators in this report, such as PDO, ONI, Copepod Biomass Anomalies and Juvenile Salmon Catch. A related quantitative model predicts a reasonable probability

Table 4.3.1 “Stoplight” table of basin-scale and local-regional conditions for smolt years 2015-2018 and projected adult returns in 2019 for coho and Chinook salmon that inhabit coastal Oregon and Washington waters during their marine phase. Green/circle = “good,” yellow/square = “intermediate,” and red/diamond = “poor,” relative to long-term time series. Courtesy of Dr. Brian Burke (NOAA).

| Scale of indicators | Smolt year | | | | Adult return outlook | |
|----------------------------------|------------|------|------|------|----------------------|---------------|
| | 2015 | 2016 | 2017 | 2018 | Coho, 2019 | Chinook, 2019 |
| Basin-scale | | | | | | |
| PDO (May-Sept) | ◆ | ◆ | ◆ | ■ | ■ | ◆ |
| ONI (Jan-Jun) | ◆ | ◆ | ■ | ● | ● | ■ |
| Local and regional | | | | | | |
| SST anomalies | ◆ | ◆ | ● | ◆ | ◆ | ● |
| Deep water temp | ◆ | ■ | ◆ | ◆ | ◆ | ◆ |
| Deep water salinity | ◆ | ■ | ● | ● | ● | ● |
| Copepod biodiversity | ◆ | ◆ | ◆ | ■ | ■ | ◆ |
| Northern copepod anomaly | ◆ | ◆ | ◆ | ● | ● | ◆ |
| Biological spring transition | ◆ | ◆ | ◆ | ◆ | ◆ | ◆ |
| Winter ichthyoplankton biomass | ● | ● | ● | ● | ● | ● |
| Winter ichthyoplankton community | ◆ | ◆ | ◆ | ◆ | ◆ | ◆ |
| Juvenile Chinook catch (Jun) | ■ | ◆ | ◆ | ■ | ■ | ◆ |

of modest increases in returns of Fall Chinook and coho relative to 2018, but comparable returns of Spring Chinook (Appendix H.3).

4.4 GROUND FISH: STOCK ABUNDANCE AND COMMUNITY STRUCTURE

Because no assessments were conducted in 2018, this year's groundfish stock indicators are identical to last year's (updated through the 2017 assessment year). All groundfish assessed from 2007-2017 were above biomass limit reference points (LRPs); thus, no stocks were considered "overfished" (Figure 4.4.1, x-axis), although previously overfished yelloweye rockfish and cowcod were still rebuilding toward target reference points. Stocks of black rockfish (in CA and WA) and China rockfish (in CA) were being fished above the fishing rate proxy in their most recent assessments from 2015 (Figure 4.4.1, y-axis). These three stocks' fishing rates appear to be over the targets due to recent changes in how the targets are calculated in the assessments, not because of changes in management or fishery practices.

This figure will be updated with the assessments done in 2019.

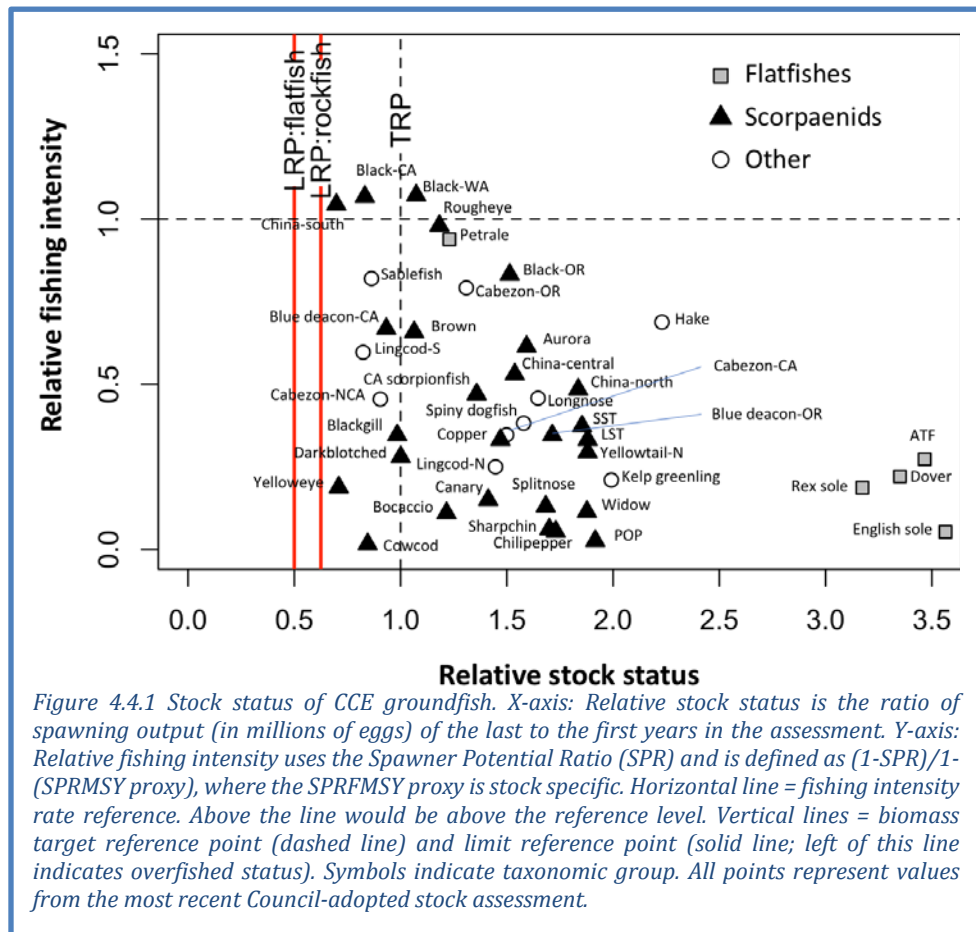
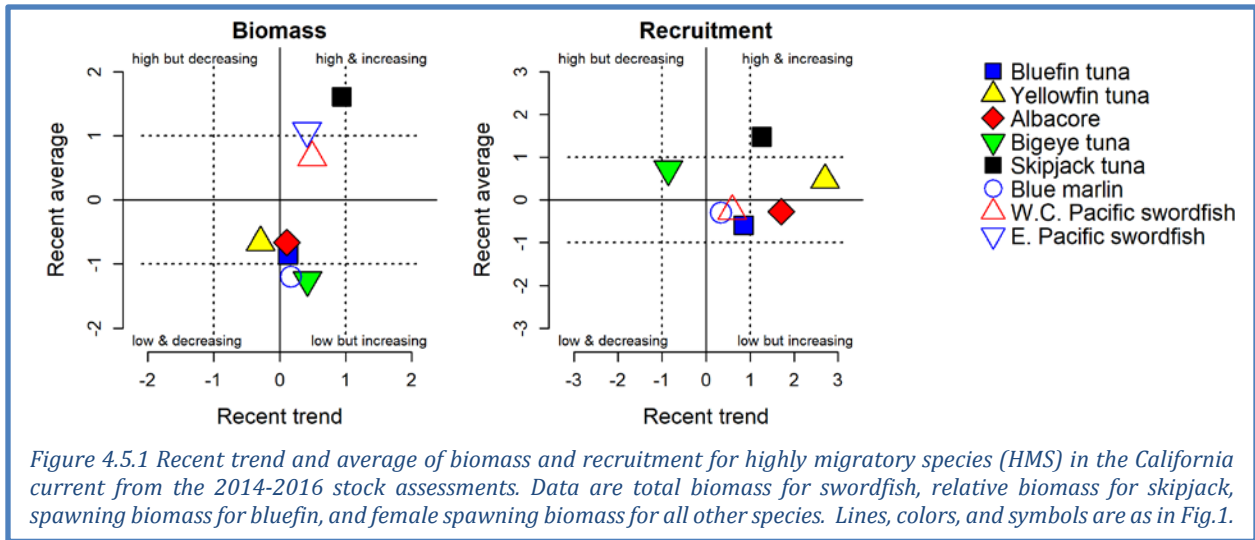


Figure 4.4.1 Stock status of CCE groundfish. X-axis: Relative stock status is the ratio of spawning output (in millions of eggs) of the last to the first years in the assessment. Y-axis: Relative fishing intensity uses the Spawner Potential Ratio (SPR) and is defined as $(1-SPR)/(1-SPR_{MSY})$ proxy, where the SPR_{MSY} proxy is stock specific. Horizontal line = fishing intensity rate reference. Above the line would be above the reference level. Vertical lines = biomass target reference point (dashed line) and limit reference point (solid line; left of this line indicates overfished status). Symbols indicate taxonomic group. All points represent values from the most recent Council-adopted stock assessment.

4.5 HIGHLY MIGRATORY SPECIES

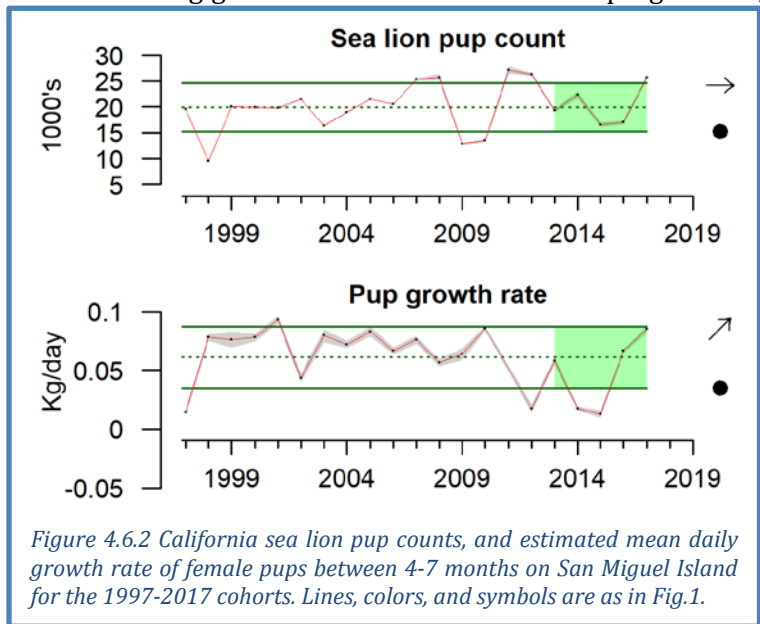
For highly migratory species (HMS), we present quad plots of recent averages and trends of biomass and recruitment from the most up-to-date stock assessment, including several species that are managed by the Council; time series and supporting documentation are found in Appendix I. The most recent assessments range from 2015-2018. Average biomass of two stocks (eastern Pacific swordfish and skipjack) over the most recent 5 years was >1 s.d. above the long-term mean, while blue marlin and bigeye tuna were >1 s.d. below their long-term means (Figure 4.5.1, left). Bigeye tuna, bluefin tuna, and blue marlin biomasses appeared to be near historic lows. Only bluefin tuna are thought to be overfished and experiencing overfishing at the scale of their full range, although uncertainty exists for other stocks, particularly bigeye tuna (Appendix I). Biomass trends were neutral for all species except skipjack, which were increasing. Recruitment indicators varied widely: recruitment appears to be increasing for skipjack and yellowfin tuna and neutral for other stocks (Figure 4.5.1, right). There was an apparent increase in age-0 bluefin in 2016 (Appendix I).



4.6 MARINE MAMMALS

Sea lion production: California sea lions are sensitive indicators of prey availability in the central and southern CCE (Melin et al. 2012): sea lion pup count at San Miguel Island relates to prey availability to gestating females from October to June, while pup growth at San Miguel from birth to age 7 months is related to prey availability to lactating females from June to February.

In 2017, pup births and growth rates showed significant improvement over 2016. Births were >1 s.d. above the long-term mean for the first time since 2012 and contrasting a declining trend in recent cohorts (Figure 4.6.1, top). The increase in births indicates that low numbers of births in 2015 and 2016 were due to the poor foraging conditions during gestation and fewer successful pregnancies, rather than a decline in survival of reproductive females. Pup growth rate was the third highest observed since 1997, and has increased since record lows in the 2014 and 2015 cohorts (Figure 4.6.1, bottom). The return of anchovy to the community and to the diet of sea lion females coincided with improved pup condition. However, the fattest pups in the time series occurred in the mid-2000s when sardine and anchovy dominated the diet, suggesting that a diverse diet with anchovy and sardine or other high-quality species like mackerel is key to supporting reproductive efforts of California sea lion females.



Whale entanglement: Coincident with the anomalous warming in 2014-2016, observations of whales entangled in fishing gear occurred at levels far greater than in the preceding decade. Reported entanglements were most numerous in 2015 and 2016, the majority involving humpbacks. Most observations occurred in California waters, although entanglement reports in 2018 were more widely dispersed along the US West Coast than in previous years. Based on preliminary data, in 2018 the number of reported entanglements increased toward the record highs seen in 2015 and 2016

after a decrease in 2017 (Figure 4.6.2). The majority of reported entanglements occur in gear that cannot be identified visually. Most of the portion that can be identified is confirmed to be Dungeness crab gear. However, in both 2016 and 2017, sablefish fixed gear was identified in at least one entanglement, and gillnets have been observed in some entanglements in every year since 2012. Many interacting factors could be causing the increased numbers of observed entanglements, including shifts in oceanographic conditions and prey fields, changes in whale populations, changes in distribution and timing of fishing effort, and increased public awareness and improved reporting.

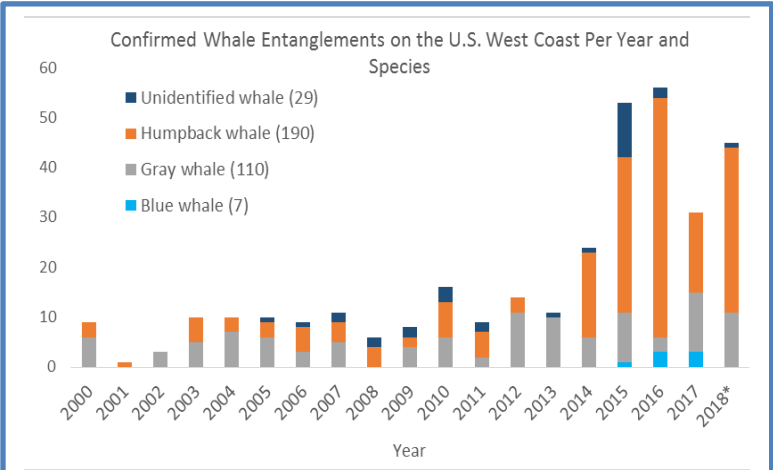


Figure 4.6.3 Numbers of whales reported as entangled in fishing gear along the West Coast from 2000-2018.

4.7 SEABIRDS

Seabird abundance indicators are assumed to reflect regional forage availability. The three bird species included here represent distinct foraging strategies and spatial ranges (Appendix J). We use a quad plot to summarize regional time series of at-sea density of these species in spring and early summer (Figure 4.7.1); time series updated through 2018 are in Appendix J.

Seabird density patterns varied by species and region. Though sooty shearwaters experienced short-term declines in both the northern and central CCE (Figure 4.7.1), their 2018 densities were substantially greater than in 2017 in all regions (Appendix J). Common murre spring densities increased in the central and southern CCE over the past 5 years, and were the highest ever recorded in the southern region in 2018. Cassin’s auklet densities declined in the northern CCE over the past 5 years and were stable elsewhere; densities in 2018 were just below average in all regions.

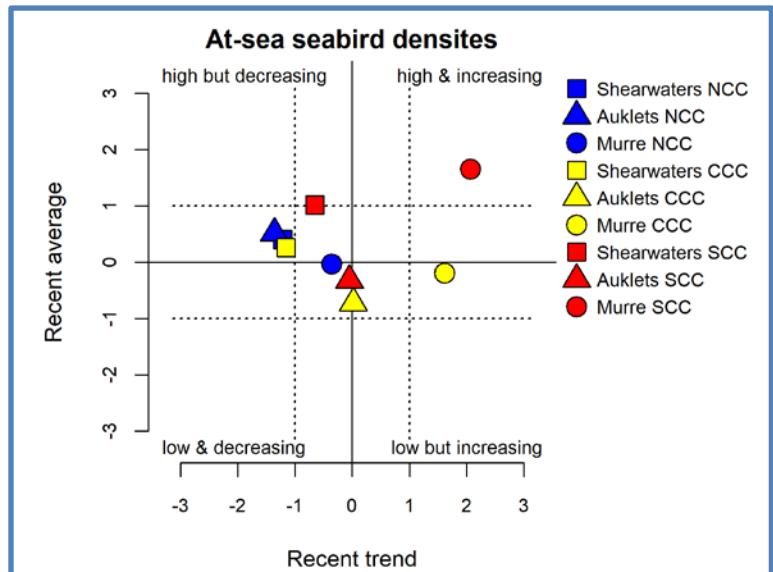


Figure 4.7.1 Recent (5-year) trend and average of seabird at-sea densities during the spring in the California Current in three regions through 2018. Lines, colors, and symbols are as in Fig.1.

In the warm and unproductive years of 2014-2016, there were major seabird mortality events (“wrecks”) of Cassin’s auklets in 2014, common murres in 2015 and rhinoceros auklets in 2016. In 2018, for the second year in a row, there were no widespread wrecks in the CCE (Appendix J.2).

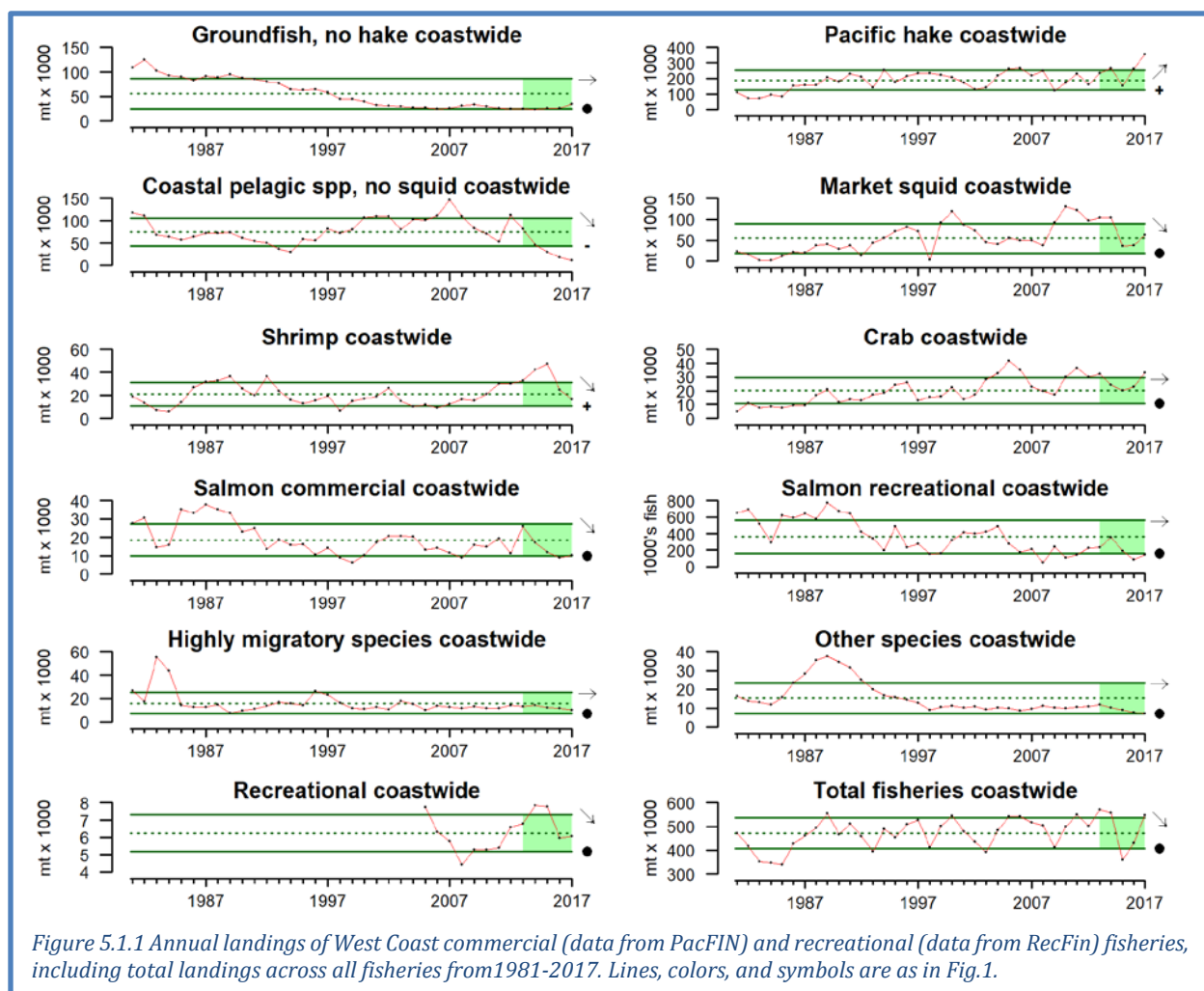
5 HUMAN ACTIVITIES

5.1 COASTWIDE LANDINGS BY MAJOR FISHERIES

Data for fishery landings are available through 2017. Coastwide landings have been highly variable in recent years, driven by steep declines in landings of CPS finfish, market squid, shrimp and salmon, coupled with large Pacific hake landings in 2016 and especially 2017 (Figure 5.1.1). Total landings increased 27.4% from 2016 to 2017. Landings of groundfish (excluding hake) were near historic lows from 2013-2017, though a slight increase occurred in 2017. Landings of CPS finfish decreased to the lowest levels in recent decades. Shrimp landings have been above average for the most recent 5-year span, despite declines in 2016 and 2017. Commercial landings of salmon have declined sharply and remained low over the last several years. Landings of HMS and other species have been within ± 1 s.d. of historic averages over the last 20+ years. State-by-state landings are presented in Appendix K.1.

Recreational landings (excluding salmon and Pacific halibut) were within historical averages for the last 5 years (Figure 5.1.1). A recent decline was due to a 70-80% decrease in yellowfin tuna and yellowtail landings in 2016. Recreational landings of Chinook and coho salmon were near the lowest levels observed in recent decades. State-by-state recreational landings are in Appendix K.1.

Total revenue for West Coast commercial fisheries in 2017 was ~ 1 s.d. above the long-term average, and 12.3% higher than 2016. The increase was driven by high revenues from Pacific hake, market squid and crab. Coastwide and state-by-state revenue data are presented in Appendix K.2.



5.2 GEAR CONTACT WITH SEAFLOOR

Benthic species, habitats and communities can be disturbed by natural processes, and also by human activities (e.g., fishing, mining, dredging). The impacts of these activities likely differ by seafloor habitat type, with hard, mixed and biogenic habitats needing longer to recover than soft sediment. Spatially explicit indicators may inform spatial management of specific human activities.

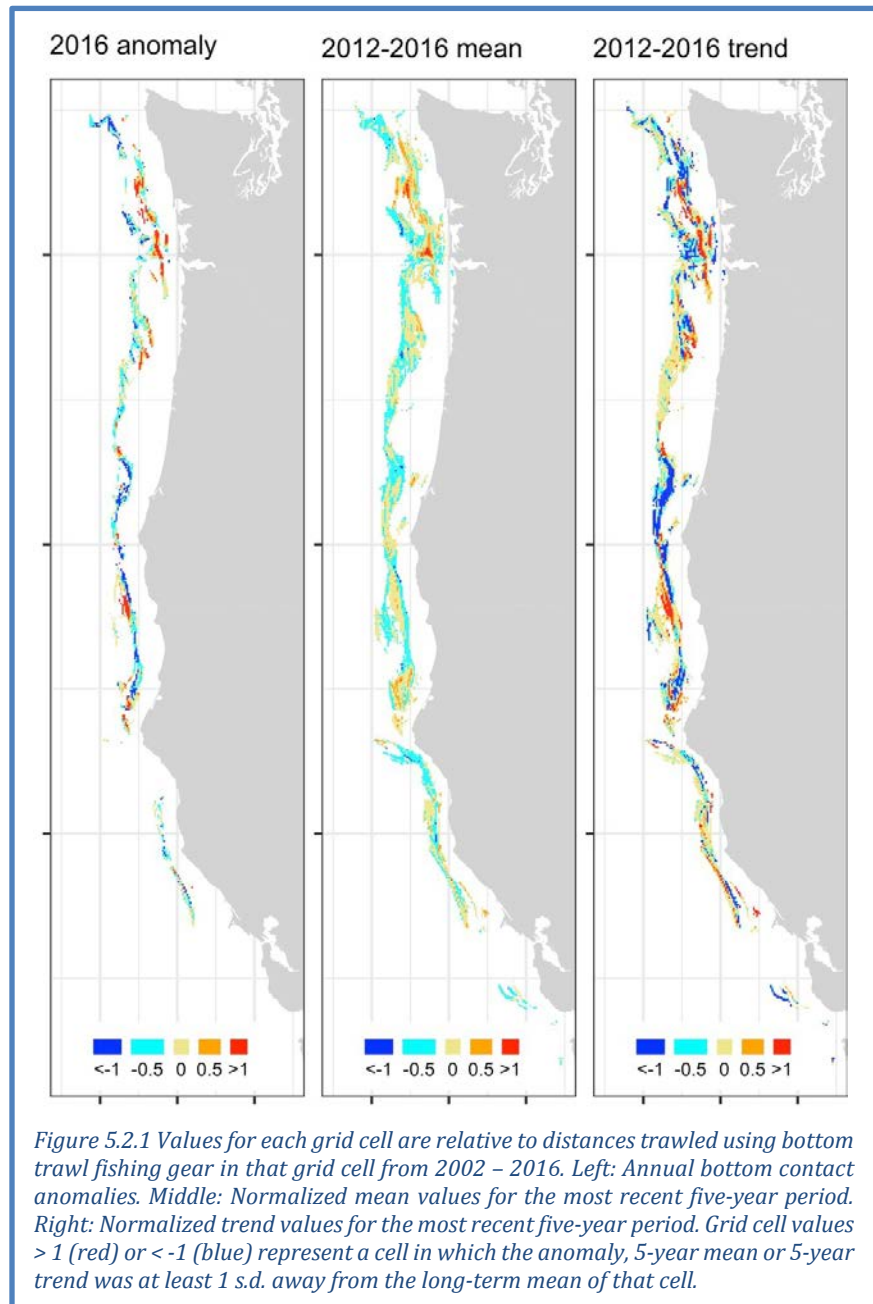
To illustrate spatial variation in bottom trawling activity, we estimated total distance trawled on a 2x2-km grid from 2002-2016. For each grid cell, we mapped the 2016 anomaly from the long-term mean, the most recent 5-year average and the most recent 5-year trend (Figure 5.2.1). Off Washington, cells where distance trawled was above average and increasing tended to be in central and southern waters (red cells), while northern cells mostly experienced below-average and decreasing trawl contact (blue cells). Off Oregon, red cells in 2016 and in the trend map were in several patches, the largest of which was off Newport, while blue cells in 2016 and the trend map were most concentrated to the north and south of Cape Blanco. Off California, the most notable patches of red cells in 2016 were just north of Cape Mendocino, while cells with increasing or decreasing trends from 2012-2016 were widespread. These spatial indicators are more informative than the coast-wide aggregated time series which showed bottom trawl contact at historically low levels and no trend from 2012 to 2016 (Appendix L).

6 HUMAN WELLBEING

6.1 SOCIAL VULNERABILITY

Coastal community vulnerability indices are generalized socioeconomic vulnerability metrics for

communities. The Community Social Vulnerability Index (CSVI) is derived from social vulnerability data (demographics, personal disruption, poverty, housing, labor force structure, etc.; Jepson and



Colburn 2013). We monitor CSVI in communities highly reliant upon both commercial fishing (Figure 6.1.1) and recreational fishing (Figure 6.1.2).

The commercial fishing reliance index is based on an analysis of variables reflecting *per capita* engagement in commercial fishing (e.g., landings, revenues, permits, and processing) in 1140 West Coast communities. Figure 6.1.1 plots CSVI in 2016 against commercial fishery reliance for communities that are most reliant on commercial fishing in Washington, Oregon, and California. Communities above and to the right of the dashed lines are those with above average levels of CSVI (horizontal dashed line) and commercial fishing reliance (vertical dashed line). For example, Port Orford and Westport have high fishing reliance (4 and 9 s.d. above average) and high CSVI (6 and 4 s.d. above average) compared to other coastal communities. Outliers in both indices may be especially socially vulnerable to commercial fishery downturns.

The recreational fishing engagement index is a similar analysis of variables reflecting a community's *per capita* recreational fishing engagement (e.g., number of boat launches, number of charter boat and fishing guide license holders, number of charter boat trips, and a count of support businesses such as

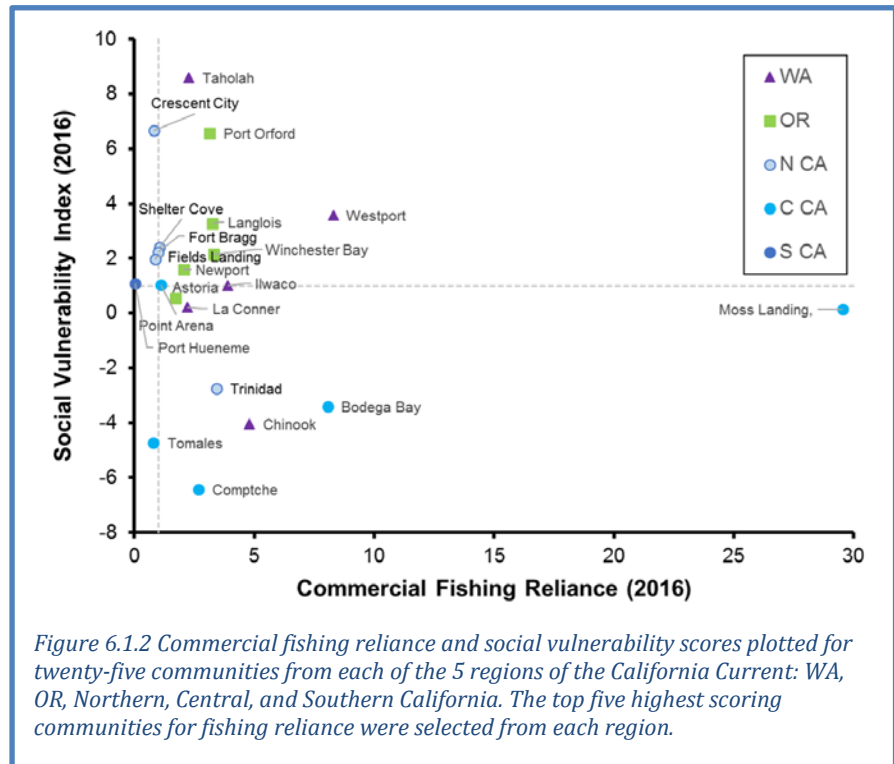


Figure 6.1.2 Commercial fishing reliance and social vulnerability scores plotted for twenty-five communities from each of the 5 regions of the California Current: WA, OR, Northern, Central, and Southern California. The top five highest scoring communities for fishing reliance were selected from each region.

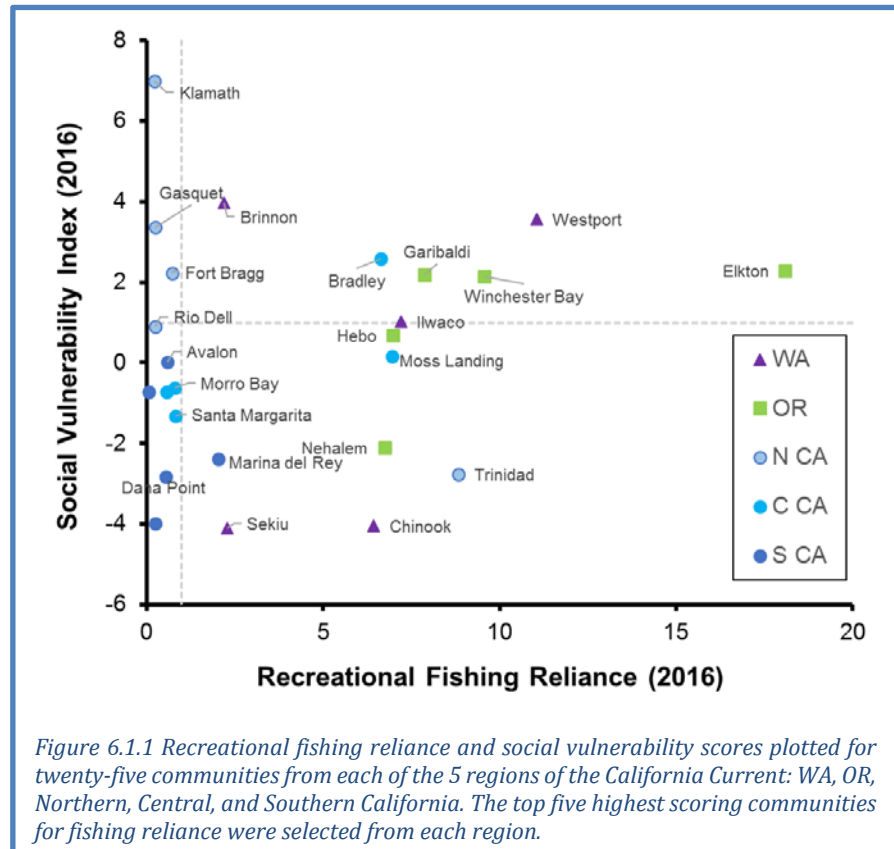


Figure 6.1.1 Recreational fishing reliance and social vulnerability scores plotted for twenty-five communities from each of the 5 regions of the California Current: WA, OR, Northern, Central, and Southern California. The top five highest scoring communities for fishing reliance were selected from each region.

bait and tackle shops). The analysis does not differentiate between marine recreational fishing and inland recreational fishing, which may include anadromous salmonids of coastal commercial and recreational interest. Figure 6.1.2 plots CSVI against recreational fishery reliance in 2016 for the five communities most reliant on recreational fishing in the same five geographic regions. Communities above and to the right of the dashed lines, such as Garibaldi and Westport, have higher-than-average recreational reliance and social vulnerability. Some communities (Westport, Ilwaco, Winchester Bay) are outliers on both axes in both the commercial and recreational plots, which may imply some potential for management-related tradeoffs in those communities.

This is an emerging area of work and more research will be required to understand the importance of these relationships. An effort to examine communities that may be particularly affected by ecosystem shifts, with respect to the Magnuson-Stevens Act's National Standard 8, is ongoing. Additional findings on these fishery engagement relationships are in Appendix M.

6.2 DIVERSIFICATION OF FISHERY REVENUES

According to the effective Shannon index (ESI) metric that we use to measure diversification of revenues across different fisheries (see Appendix N), the fleet of 28,000 vessels that fished the West Coast and Alaska in 2017 was essentially unchanged from 2016 for most vessel classes, but was less diverse on average than at any time in the prior 36 years (Figure 6.2.1a). Most vessel categories have been trending down for several years, notably the California fleet and the largest vessels coastwide (Figure 6.2.1b, d). The

long-term decline in fishery diversification is due both to entry and exit of vessels, and to changes for individual vessels. Less diversified vessels have been more likely to exit, vessels that remain in the fishery have become less diversified since the mid-1990s, and newer entrants have generally been less diversified than earlier entrants. Within the average trends, there are wide ranges of diversification levels and strategies, and some vessels remain highly diversified. Increased diversification from one year to the next may not always indicate an improvement. For example, if a class of vessels was heavily dependent on a single fishery with highly variable revenues (e.g., Dungeness crab), a decline in that fishery might force vessels into other fisheries, causing diversification to increase. Also an increase in a fleet's diversification may be due less diversified vessels exiting (Appendix N).

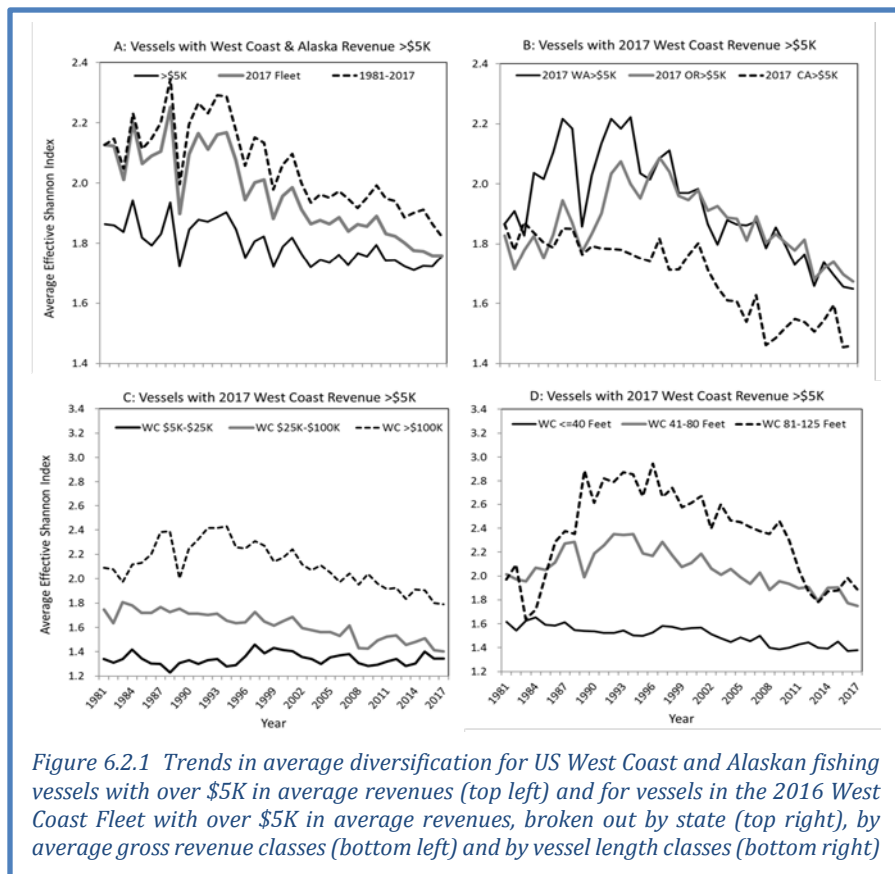
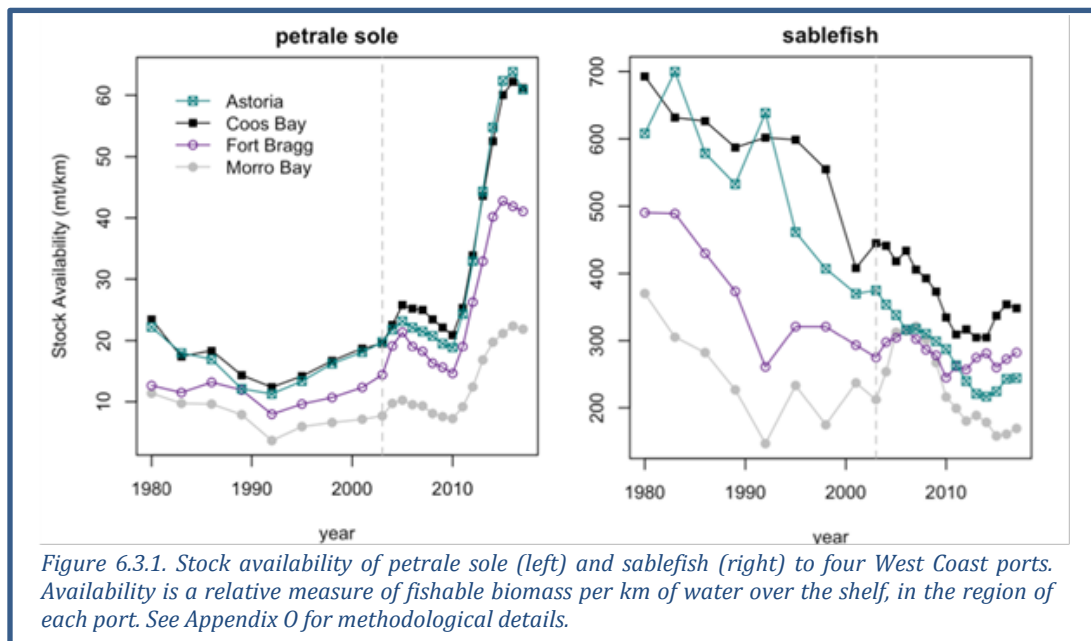


Figure 6.2.1 Trends in average diversification for US West Coast and Alaskan fishing vessels with over \$5K in average revenues (top left) and for vessels in the 2016 West Coast Fleet with over \$5K in average revenues, broken out by state (top right), by average gross revenue classes (bottom left) and by vessel length classes (bottom right)

6.3 STOCK SPATIAL DISTRIBUTION AND AVAILABILITY TO PORTS

Fishing communities must contend with changes in availability of important target stocks. Changes in availability may happen due to changes in the stock's population size, changes in its distribution, or both. To determine how fishing communities along the US West Coast experience changes in the distribution of fish stocks, we estimated fluctuations in the relative availability of two groundfish species (petrale sole and sablefish) to four communities (Astoria, Coos Bay, Fort Bragg, and Morro Bay) from 1980-2017 (Figure 6.3.1). This stock availability index represents the cumulative effects of changes in biomass (based on stock assessment output) and shifts in spatial distribution (based on VAST model output; methods details in Appendix O). While the qualitative trends in stock availability reflect trends in biomass reported in stock assessments, the four communities represented here experienced those trends quite differently depending on where they occur along the coast.

The coastwide biomass of sablefish declined more than 50% since 1980, but the distribution of sablefish is centered further south today than it was in the early 1990s. This change in the center of gravity of the stock has counteracted the decline in sablefish biomass for southern ports (Fort Bragg and Morro Bay) over the last 25 years, such that stock availability was relatively stable compared to Astoria and Coos Bay. In contrast, while the biomass of petrale sole has increased everywhere along the coast since the early 2000s, the center of gravity of this stock is now farther north than it was historically. Thus, relative stock availability has tripled for Astoria and Coos Bay but increased more modestly for Fort Bragg and Morro Bay.



Ecological, technological, management, economic, governance, and other social factors influence the availability of target species to fishing communities. This same set of considerations influences the capacity of these communities to respond to shifting availability of target species. Climate variability and change, in particular, challenge the capacities of fishing communities to keep pace with shifts in stock availability. Analyses like those presented here represent a first step toward evaluating the impacts of changing social and ecological conditions on the availability of target species and the individual fishing communities that depend upon them. In the future, this analysis can be updated annually for any west coast community and for groundfishes well-sampled by the trawl survey, and can focus on the attribution of potential causes underlying the shifts in availability observed here.

7 SYNTHESIS

7.1 SUMMARY OF RECENT CONDITIONS

Over the past two years, the CCE appears to have been in a slow transition away from the anomalous, warm, and relatively unproductive conditions of 2014-2016 (e.g., Thompson et al. 2018). Within our indicators, this slow transition is demonstrated by:

- Basin-scale climate indices, such as mostly neutral ONI and PDO values
- Regional environmental indicators (generally average upwelling, snowpack, stream flow)
- Indicators of productivity of lower trophic levels (relatively average copepod community composition off Newport and krill size off northern California, subtle improvements in salmon indicators, no evidence of recent HABs off Washington, increases in anchovy)
- Indicators of predator foraging (improving conditions for sea lion pups, average or increasing densities of piscivorous seabirds)
- Recent increases in landings and revenues in several FMPs

Furthermore, some variables that we had expected to be negatively affected by the warm conditions in 2014-2016 actually exceeded those expectations, notably the large numbers of juvenile groundfish caught in pelagic surveys, suggesting that some parts of the CCE were resilient to the direct influence of the anomalous conditions.

However, referring to the last few years as “a slow transition” begs the question: a transition to what? We do not know the answer to that, as there are neither definitive signs that the CCE will resume the productive conditions experienced for several years prior to 2014, nor definitive signs that the CCE will move back to a relatively unproductive state. Moreover, many indicators suggest lingering effects of the anomalies of 2014-2016, including persistence of subsurface warm water, high concentrations of pyrosomes, and whale entanglements in fishing gear. Other concerning signs include persistently low NPGO anomalies, widespread hypoxic events, episodes of northeast Pacific warming (see Figure 3.1.3), and loss of fishery diversification. Our uncertainty about where this “transition” is leading underscores the importance of continued careful monitoring, modeling and analysis of indicators at appropriate scales; refinement of forecasting tools (see below); and maintaining communication between scientists, managers, and stakeholders.

7.2 FORECASTS AND PREDICTIONS FOR 2019

In March 2015, the Council approved FEP Initiative 2, “Coordinated Ecosystem Indicator Review” (Agenda Item E.2.b), by which the Council, advisory bodies, the public, and the CCIEA team would work jointly to refine the indicators in the annual CCIEA Ecosystem Status Report to better meet Council objectives. Many of the recommendations of that 2-year process have already been implemented over the past several iterations of this report, including the current report for March 2019 (for examples, see Appendix C). One of the priorities identified by several advisory bodies was that the CCIEA team develop and evaluate leading indicators and analyses that support short-term forecasting. We therefore will conclude the main body of this year’s report with information that may provide insight on conditions that will occur in 2019.

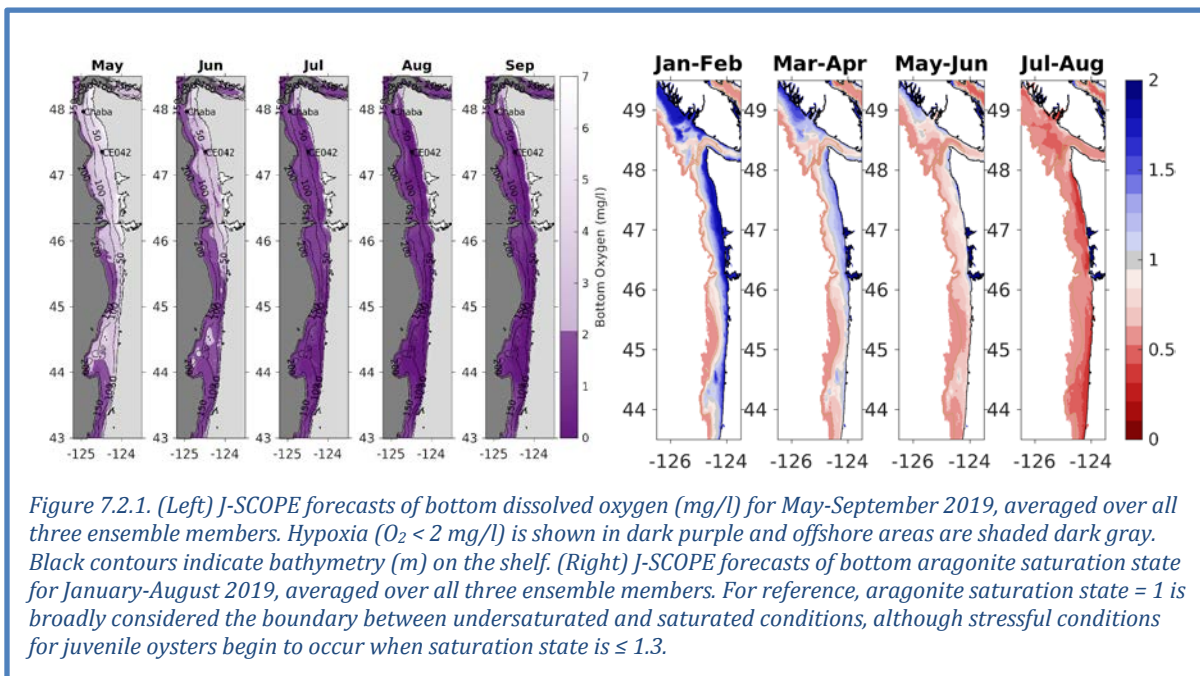
Some sections above have indicators and analyses that provide forecasting ability. These are:

- **El Niño forecast (Section 3.1).** The NOAA Climate Prediction Center predicts a 65% chance that a mild El Niño will form in the equatorial Pacific at least through spring 2019.
- **Salmon returns to the Columbia River and Oregon Production Index area (Section 4.3).** The indicator “stoplight chart” and related quantitative analyses predict below-average returns of Chinook salmon to Bonneville Dam in 2019, and moderate survival of coho salmon returning to Oregon coastal systems in 2019.

An additional set of forecasting tools has been developed in a partnership between academic scientists and CCIEA team members, and were reviewed in September 2018 by the SSC Ecosystem Subcommittee. The **J-SCOPE forecast system** (www.nanoos.org/products/j-scope) provides short-term skilled forecasts of ocean conditions off of Washington and Oregon, and these forecasts have been extended to include seasonal predictions of habitat quality for sardines (Siedlecki et al. 2016, Kaplan et al. 2016). Each January, the J-SCOPE modelers produce an ensemble of 3 forecasts that span January-September and include variables like temperature, dissolved oxygen, chlorophyll, aragonite saturation state (ocean acidification), and sardine habitat, in addition to other dynamics such as the timing and intensity of upwelling.

According to the J-SCOPE ensemble forecast of the 2019 summer upwelling season (May-August):

- Sea surface temperatures are expected to be higher than average, with warm anomalies extending below the surface (related to the El Niño forecast)
- Dissolved oxygen on the bottom declines over the course of the forecast, with hypoxia (<2 mg/L) prominent over the Oregon shelf in June and spreading to Washington by July (Figure 7.2.1, left). Compared to previous years, oxygen is expected to be lower than average in Washington and near average in Oregon. The relative uncertainty in the forecast remains low (10%) until the end of the upwelling season (July-August), when it increases to $\sim 50\%$
- Aragonite on the bottom is expected to be undersaturated (i.e., more corrosive) throughout the upwelling season for most of the region except for shallow nearshore Washington shelves (Figure 7.2.1, right); surface waters are expected to be supersaturated throughout the season
- Chlorophyll-a concentrations are forecast to be below average early in the upwelling season; later, chlorophyll is forecast to be above average over the Washington shelf and Heceta Bank, but below average over the rest of the Oregon shelf
- Waters throughout the region are expected to be suitable for sardine (if they are present)



Forecasts for temperatures, chlorophyll and sardines can be viewed at the J-SCOPE website, <http://www.nanoos.org/products/j-scope/forecasts.php>. Additional species forecasts are being developed and will be available in future years.